Revisão

HYDROGEN PRODUCTION BY ALKALINE WATER ELECTROLYSIS

Diogo M. F. Santos* and César A. C. Sequeira
Materials Electrochemistry Group, ICEMS, Instituto Superior Técnico, TULisbon, Av. Rovisco Pais, 1049-001 Lisboa, Portugal
José L. Figueiredo
Laboratório de Catálise e Materiais (LCM), Laboratório Associado LSRE/LCM, Departamento de Engenharia Química, Faculdade de Engenharia, Universidade do Porto, R. Dr. Roberto Frias, 4200-465 Porto, Portugal

Water electrolysis is one of the simplest methods used for hydrogen production. It has the advantage of being able to produce hydrogen using only renewable energy. To expand the use of water electrolysis, it is mandatory to reduce energy consumption, cost, and maintenance of current electrolyzers, and, on the other hand, to increase their efficiency, durability, and safety. In this study, modern technologies for hydrogen production by water electrolysis have been investigated. In this article, the electrochemical fundamentals of alkaline water electrolysis are explained and the main process constraints (e.g., electrical, reaction, and transport) are analyzed. The historical background of water electrolysis is described, different technologies are compared, and main research needs for the development of water electrolysis technologies are discussed.

Keywords: alkaline water electrolysis; cell components; hydrogen production.

INTRODUCTION

Hydrogen, as an energy carrier, has become increasingly important, mainly in the last two decades. It owes its popularity to the increase in the energy costs caused by the uncertainty in the future availability of oil reserves[1] and also to the concerns about global warming and climate changes, which are blamed on manmade carbon dioxide emissions associated with fossil fuel use,[2] particularly coal.[3] Hence, despite the cost of hydrogen being still higher than most fossil fuels, its unique set of properties is finding new applications in many directions: hydrogen-fuelled forklifts are being used in enclosed spaces, different types of fuel cells (FCs) are being used in power production, major cities have implemented hydrogen-fuelled buses, FCs for electronic devices and mobile phones are close to commercialization; Germany is manufacturing and selling hydrogen-fuelled submarines, some companies are experimenting on hydrogen-fuelled sea-going vessels, and hydrogen FCs are being considered in aerospace applications.[4]

Today, these major changes in our society have led hydrogen producers and some petroleum companies to establish hydrogen-fuelling stations throughout Japan and Germany. Major car companies are planning to start selling hydrogen-fuelled cars in Germany, Japan, and those places where there are enough hydrogen-fuelling stations, in 2–3 years' time.[4] Clearly, hydrogen has been perceived as a valid alternative to fossil fuels in many applications because of its advantage of being a clean fuel, considering that its use emits almost nothing other than water. Additionally, it can be produced using any energy source, with renewable energy being most attractive,[5] making it one of the solutions to sustainable energy supply in the so-called new "hydrogen economy."[6,7]

Notwithstanding the increasing interest in hydrogen as an energy carrier, its main uses continue to be in petroleum refining, ammonia production, metal refining, and electronics fabrication, with an average worldwide consumption of about 40 million tonnes.[8–13] This large-scale hydrogen consumption consequently requires large-scale hydrogen production. Presently, the technologies that dominate hydrogen production include reforming of natural gas,[14] gasification of coal and petroleum coke,[15,16] as well as gasification and reforming of

heavy oil.[17,18] Although water electrolysis has been known for around 200 years,[19,20] it still contributes only a minor fraction of the total hydrogen production (4% of the worldwide hydrogen production).[21,22] When compared to other available methods, water electrolysis has the advantage of producing extremely pure hydrogen (>99.9%), ideal for some high value-added processes such as manufacture of electronic components.[13] Water electrolysis is often limited to small-scale applications and to particular cases where large-scale hydrogen production plants are not accessible or economical to use. These include marine, rocket, spacecraft, electronic, and food industries, as well as medical applications.

Water electrolysis works well at a small scale, and the process is even more sustainable if electricity used is derived from renewable sources (e.g., wind, solar, hydro, etc.). In a conceptual energy system involving production, conversion, storage, and use in remote communities, water electrolysis may play an important role. When abundant renewable energy is available, extra energy may be stored in the form of hydrogen using water electrolysis. The stored hydrogen can then be used in FCs to generate electricity or used as a fuel gas for heating applications. Therefore, electricity generated by the renewable energy is either directly merged into the grid or used to produce hydrogen. Figure 1 illustrates such an energy system.
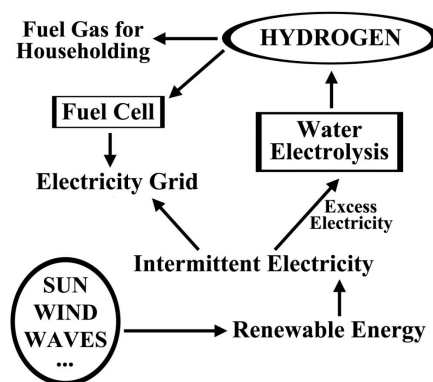

Figure 1. *Conceptual energy system using water electrolysis to produce hydrogen for use as a fuel gas or an energy storage medium*

*e-mail: diogosantos@ist.utl.pt

Remote areas with abundant solar and/or wind resources for generating electricity can take advantage of water electrolysis to produce hydrogen to meet the energy needs of household applications such as lighting and heating,[23] for powering telecommunication stations,[24] for applications in small-scale light-manufacturing industry, for electricity peak shaving, and in integrated systems, both grid connected and grid independent.[25] Hydrogen produced by renewable energy sources has the advantage of mobility, which is essential for supplying energy in remote areas away from the main electricity grid.

Small-scale water electrolyzers may avoid the need for a large number of cryogenic, liquid hydrogen tanks or a huge hydrogen pipeline system. The existing electrical power grid can be used as the backbone of the hydrogen infrastructure system, contributing to the load leveling by changing operational current density in accordance with the change in electricity demand.[26] Small-scale water electrolyzers may be used to produce pure hydrogen and oxygen for diverse applications, such as use of hydrogen gas in laboratories and oxygen in life-support systems in hospitals.[27] It has been shown that for small systems, the dominant factor in determining the cost of electrolytic hydrogen is the cost of the electrolysis cells, whereas for large systems electricity cost and hydrogen value dominate the discussion.[13]

Although hydrogen possesses the advantages of availability, flexibility, and high purity, for its widespread applications hydrogen production using water electrolysis needs improvements in energy efficiency, safety, durability, operability, and portability, and, above all, reduction in installation and operation costs. These features open up many opportunities for research and development leading to technological advancements in water electrolysis. This paper presents the electrochemical fundamentals of water electrolysis and a theoretical basis for scientific analysis of the available electrolysis systems. The various water electrolysis techniques and a broad range of applications are analyzed. The main research needs are identified and future trends are discussed.

HISTORICAL BACKGROUND

From the discovery of the phenomenon of electrolytic splitting of water into hydrogen and oxygen to the development of modern electrolyzers, water electrolysis technology has seen continuous progresses over the past 200 years.[28] Following the discovery of electricity, J.R. Deiman and A.P. van Troostwijk, in 1789, used an electrostatic generator to discharge electricity through two gold wires placed inside a tube filled with water, causing evolution of gases.[29] Alessandro Volta invented the voltaic pile in 1800, and a few weeks later William Nicholson and Anthony Carlisle used it for electrolytic splitting of water.[30] Later, the gases produced during water electrolysis were identified to be hydrogen and oxygen. With the development of electrochemistry, the proportional relationship between electrical energy consumption and the amount of gases produced became established through Faraday's law of electrolysis. Finally, the concept of water electrolysis was defined scientifically and acknowledged.[31] With the invention of the Gramme machine in 1869 by Zénobe Gramme, water electrolysis became an economical method of producing hydrogen. A technique for industrial synthesis of hydrogen and oxygen through water electrolysis was developed later in 1888 by Dmitry Lachinov. By 1902, more than 400 industrial water electrolyzers were already in operation.[30] Figure 2 illustrates such early plants used for water electrolysis.[32]

The period between the 1920s and the 1970s was the "golden age" for the development of water electrolysis technology,[28] when most of the traditional designs were created. Driven by the industrial need for hydrogen and oxygen, the knowledge established in the first stage was applied to the industrialization of water electrolysis
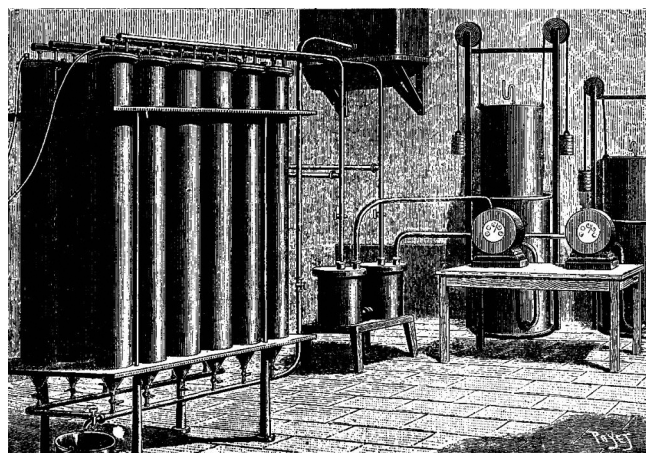

Figure 2. *Early plants for the industrial electrolysis of water*[32]

technologies. In 1939, the first large water electrolysis plant, with a capacity of 10,000 N m^3 H_2 h^{-1}, went into operation, and in 1948, the first pressurized industrial electrolyzer was manufactured by Zdansky/Lonza.[30] Commercial water electrolysis concepts developed in this period include most of the technological components that are currently in use.[33] One of these components is the membrane. The first membranes to be commercialized were made of asbestos. However, asbestos is not very resistant to corrosion caused by a strongly alkaline environment at high temperatures. Moreover, due to its seriously adverse health effects, asbestos was gradually replaced by other materials.[34] From the 1970s onward, polymers based on perfluorosulfonic acid, arylene ether, or polytetrafluoroethylene have been used as gas separation material.[34,35]

Configuration of the water electrolysis cell also underwent several improvements through time. Typical conventional tank cells, with a unipolar configuration, are simple, reliable, and flexible. On the other hand, filter press cells, with a bipolar configuration, have lower Ohmic losses and are more compact. High-pressure water electrolyzers, which use the bipolar configuration, would be difficult to accomplish with unipolar cells. Disadvantages of the bipolar cells are related to their structural complexity, requirement of electrolyte circulation, and use of gas/electrolyte separators.[36,37]

The electrode material selected should have good corrosion resistance, high conductivity, high catalytic effect, and low price.[38] Stainless steel and lead were pointed out as cheap electrode materials, with low overpotentials, but these cannot tolerate highly alkaline environments. Noble metals were found to be too expensive to be used as bulk electrode materials. Ni was then recognized as an electroactive cathode material with good corrosion resistance in an alkaline solution (when compared to other transition metals) and rapidly became popular during the development of water electrolyzers. Ni-based alloys have then started to be the object of extensive research efforts.[39–41]

These progresses motivated commercialization of water electrolyzers. The first records of commercial water electrolysis date back to 1900, when the technique was still in its early life. Two decades later, large-size electrolysis plants, rated at 100 MW, were developed in Canada, primarily to feed the ammonia fertilizer industries.[42] In the late 1980s, Aswan installed 144 electrolyzers with a nominal rating of 162 MW and a hydrogen generation capacity of 32,400 m^3 h^{-1}. The Brown Boveri electrolyzer is another highly modularized unit, which is able to produce hydrogen at a rate of about 4300 m^3 h^{-1}. Stuart Cell (Canada) is a well-known unipolar tank-type cell manufacturer. Hamilton Sundstrand (USA), Proton Energy Systems (USA), Shinko Pantec (Japan), and Wellman-CJB (UK) manufacture the latest proton exchange membrane (PEM) electrolyzers.

In the first half of the 20th century, there was a huge demand for hydrogen in the production of ammonia fertilizers. This need for hydrogen stimulated the development of water electrolysis technology, which was helped by the low cost of hydroelectricity at the time. However, then hydrocarbon energy started to be applied massively in industry. Hydrogen could be produced in large scale through coal gasification and natural gas reforming, and at much lower costs, gradually fading the economic advantage of water electrolysis. At that point, progresses on water electrolysis for hydrogen production simply ceased.

The oil crisis of the 1970s renewed the worldwide interest in water electrolysis.[1] In the new hydrogen economy ideology, hydrogen was being considered to be the energy carrier of the future and the key to solve the problem of sustainable energy supply. Improving the efficiency of water electrolysis became a major goal. Novel breakthroughs were achieved at the cell level, with the emergence of PEM and pressurized water electrolyzers.[43]

Compact, high-pressure water electrolyzers were used to produce oxygen on board the nuclear-powered submarines, as part of the life-supporting system. The compact design eliminates the gaskets between cells, requiring high-precision machining of the cell frames. However, high operating pressures of these water electrolyzers (up to 3.5 MPa) create a major safety problem.[1]

In 1966, General Electric for the first time used a Nafion membrane to supply energy for space projects.[43] The PEM discovery enabled the development of PEM water electrolysis, also named as solid polymer electrolysis (SPE), whose operation principles are basically the reverse of a PEM FC.[44] Intensive studies were carried out to reduce the membrane cost.[45] In the early 1970s, small-scale PEM water electrolyzers were used for space and military applications. However, the short durability of the membrane makes PEM electrolyzers too expensive for general applications.[44] A PEM water electrolysis system may offer greater energy efficiency, higher production rates, and more compact design than traditional alkaline water electrolysis technologies.[46,47] However, special requirements are needed for several of its components (e.g., expensive polymer electrolyte membrane, porous electrodes, and current collectors), which are its serious disadvantages.[25]

Currently, many efforts are under way to integrate renewable energy technologies as energy sources in water electrolysis for hydrogen production, as a means for distributed energy production, storage, and use, particularly in remote communities. New water electrolysis concepts, such as photovoltaic (PV) electrolysis and steam electrolysis, are now emerging.

FUNDAMENTALS OF WATER ELECTROLYSIS

Figure 3 presents the simplest water electrolysis unit, consisting of an anode and a cathode connected through an external power supply and immersed in a conducting electrolyte. A direct current (DC) is applied to the unit; electrons flow from the negative terminal of the DC power source to the cathode, where they are consumed by hydrogen ions (protons) to form hydrogen atoms. In the general process of water electrolysis, hydrogen ions move toward the cathode, whereas hydroxide ions move toward the anode. A diaphragm is used to separate the two compartments. Gas receivers are used to collect hydrogen and oxygen gases, which are formed at the cathode and anode, respectively (Figure 3).

For the case of water electrolysis in an acid or neutral aqueous electrolyte, the processes that occur at the electrodes' surface are described by Eqs. 1 and 2:
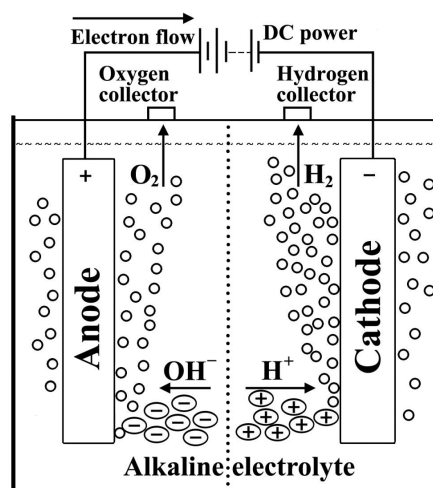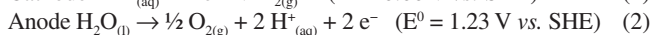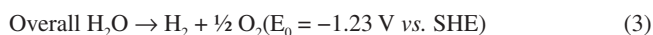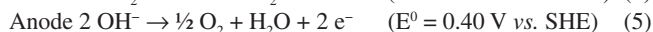
Cathode $2\,H^+_{(aq)} + 2\,e^- \rightarrow H_{2(g)}$ ($E^0 = 0.00$ V *vs.* SHE)   (1)

Anode $H_2O_{(l)} \rightarrow \frac{1}{2}\,O_{2(g)} + 2\,H^+_{(aq)} + 2\,e^-$ ($E^0 = 1.23$ V *vs.* SHE)   (2)

Figure 3. *Basic scheme of a water electrolysis system*

The sum of these two equations leads to the overall reaction of water electrolysis, as given in Eq. 3.

Overall $H_2O \rightarrow H_2 + \frac{1}{2}\,O_2$($E_0 = -1.23$ V *vs.* SHE)   (3)

However, for the specific case of alkaline water electrolysis, where a strong base is used as the electrolyte, the hydroxide anions are transferred through the electrolyte to the anode surface, where they lose electrons that then return to the positive terminal of the DC power source. Nickel (Ni) is a popular choice due to its low cost, good activity, and easy availability.[48] To enhance conductivity, the electrolyte used in the cell should consist of high-mobility ions.[49] Potassium hydroxide (KOH) is normally used in alkaline water electrolysis, thus avoiding the corrosion problems caused by acid electrolytes.[42] KOH is preferred over sodium hydroxide (NaOH) because the former electrolyte solutions have higher conductivity.[50] Therefore, when the process is run in an alkaline electrolyte, the electrochemical reactions occurring at the cathode and anode are given by Eq. 4 and Eq. 5, respectively:

Cathode $2\,H_2O + 2\,e^- \rightarrow H_2 + 2\,OH^-$ ($E^0 = -0.83$ V *vs.* SHE) (4)

Anode $2\,OH^- \rightarrow \frac{1}{2}\,O_2 + H_2O + 2\,e^-$ ($E^0 = 0.40$ V *vs.* SHE)   (5)

Of course the sum of Eqs. 4 and 5 will lead to the same overall reaction as described in Eq. 3, with the same value (-1.23 V) for the theoretical cell voltage. For these reactions to proceed, a number of barriers have to be overcome, which depend on the electrolysis cell components: the boundary layers at an electrode surface, electrode phase, electrolyte phase, separator, and electrical resistances of the circuit. Clearly, the performance of the electrolytic system must involve the understanding of the cell components. Therefore, it is appropriate to discuss them, at least in a relatively simple way.

Boundary layers at an electrode surface

The electrolytic reactions just described are heterogeneous reactions, i.e., they take place at the boundary between the electrode phase (often a solid metal or a carbonaceous material) and the electrolyte phase (often an aqueous salt solution). The discontinuous "interphase" region experiences differences in electrolyte velocity, concentration of electroactive species, and electrical potential with distance from the electrode. Each of these gradients gives rise to a different boundary layer near the electrode surface and to different physical consequences. It is most important to appreciate the nature

Table 1. Boundary layers at an electrode surface

Boundary layer	Variable	Driving force	Typical dimensions
Electrical double layer	Electrical potential	Charge separation	Molecular, i.e., $<5 \times 10^{-9}$ m
Concentration boundary layer (diffusion layer)	Reactant or product concentration	Diffusion	$<10^{-4}$ m
Hydrodynamic boundary layer (Prandtl layer)	Velocity of electrolyte	Convection	$<10^{-3}$ m

of the phenomenon resulting from the gradients and the typical extent of each boundary layer (Table 1).

The hydrodynamic and concentration boundary layers lead to mass transfer of reactants and products within the solution and will be discussed later; here the focus is on a simplified treatment of the electrical double layer resulting from the potential gradient. The electrical double layer is localized over molecular dimensions at the electrode/electrolyte interface. It arises from the charge separation between an electrode and the surrounding electrolyte. Figure 4a shows a greatly simplified model of the double layer for the case of a negatively charged electrode surface, i.e., one having a surplus of electrons.
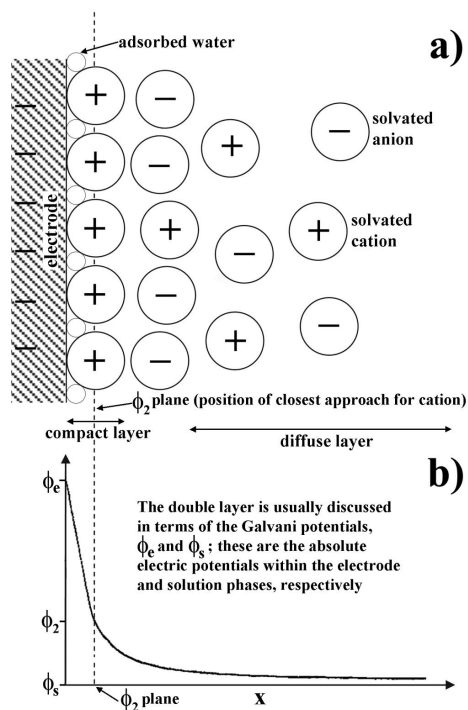
Figure 4. Electrical double layer near a negatively charged electrode surface. a) A simplified schematic of its structure. b) Potential vs. distance profile

The inner, or "compact," layer consists of cations that are electrostatically held at the electrode surface and adsorbed solvent molecules. Outside of this highly structured layer lies the "diffuse" layer where the ions retain a structure that is higher in degree than that of the bulk electrolyte. The potential field resulting from this model is shown in Figure 4b. The potential decays linearly over the compact layer and then exponentially over the diffuse layer. The system behaves as two capacitances in series, one for the compact and another for the diffuse layers.

The presence of double layer has several important consequences: (i) the difference in potentials between the electrode and solution phases, $\phi_e - \phi_s$, provides the driving force for an electron transfer reaction across the interface; (ii) this driving force may be affected significantly by adsorption of species (reactants, products, solvent, ions, or contaminants) at the electrode surface; (iii) local differences in $\phi_e - \phi_s$ may alter the localized driving force for reaction and hence

the rate, current efficiency, or selectivity of an electrode process; (iv) the potential difference across the interface is localized over molecular distances, causing the potential gradient to be extremely large, for example, if $\phi_e - \phi_s$ is equal to 2 V, over 0.2 nm, the potential gradient will be 10^{10} V m^{-1}; such a high and localized driving force enables energetically difficult processes to be carried out electrochemically; and (v) the double-layer capacitance measurements can provide useful information on adsorption at electrodes; however, it tends to create problems in kinetic studies, particularly at high-surface-area electrodes, and in case of rapid potential changes with time due to the existence of charging currents. In case of large electrodes used in industrial reactors, power supplies must be designed and controlled to handle start-up, shut-down, and other conditions where the electrode potential changes abruptly.

In the section devoted to the rate of electrode processes, kinetic expressions will be written in terms of the electrode potential, E, which is the difference between the potentials of a working electrode and a reference electrode located close to its surface in the solution. Any change in electrode potential, ΔE, can be determined from a change in potential difference across the interface, i.e., $\Delta E = \Delta (\phi_e - \phi_s)$.

Electrode phase

Both electrodes in a cell must have adequate mechanical strength and be resistant to erosion and other types of physical attacks by the electrolyte, reactants, and products. The physical form of the electrodes is often very important, as it must be readily accommodated within a selected reactor design to achieve sound electrical connections and can also be removed for inspection and maintenance. The shape and condition of the surface of an electrode should be designed taking into account the need for product separation such as disengagement of gases or solids. In many cases, there is a need to maintain a high surface area, a structure having turbulence-promoting properties, or a porous matrix having a reasonably low pressure drop. The active electrode material may also be a thin coating rather than the surface of a bulk material. The electrode surface has to achieve and maintain the desired reaction and, in some cases, must possess specific electrocatalytic properties that are essential to promote a high reaction rate for the product of interest at a low overpotential, while inhibiting all competing chemical changes. The electrical conductivity must be reasonably high throughout the electrode system, including the current feeder, electrical contacts, and the entire electrode surface, in order to avoid voltage penalties, generation of unwanted heat, as well as uneven current distribution.

Finally, the electrode performance must be obtained at a reasonable capital cost and maintained over an acceptable lifetime, possibly for several years. Some of the most common electrode materials used as cathodes for the hydrogen evolution reaction (HER) are steel, stainless steel, high-area Ni on steel, and Ni and those used as anodes for the oxygen evolution reaction (OER) are Ni oxides, and Ni- and Co-based spinels, e.g., $NiCo_2O_4$ on Ti.

Electrical resistivity is a key property of electrode materials and electrode structures. For a homogeneous material with a uniform cross-sectional area A, and resistance R, over its length L, the electrical resistivity is defined as $\rho_e = RA/L$, with the electrical conductivity

being the reciprocal of ρ_e and usually defined as k = CL/A, where the conductance, C, is the reciprocal of resistance R.

The electrical resistivity ρ_e determines the size of the potential drop through the electrode, which, in turn, contributes to power costs, possible heating problems, and a less uniform potential distribution. Typical ρ_e values for materials commonly used in electrode structures are provided in Figure 5. Only the most conducting materials, such as copper and aluminum, can be used for extensive electrical connections and current-carrying busbars. In the case of current feeders, high thermal conductivity is also useful in dissipating heat to the surroundings, as the electrical resistivity of most solid conductors increases with temperature. Costs and weights are also important; solid aluminum busbars (which sometimes have copper cores), copper or brass interelectrode connectors, or copper-cored flexible cables are used as appropriate. The passive film that forms on the external aluminum surface helps avoid corrosion but can lead to high-resistance connections if precautions are not taken.
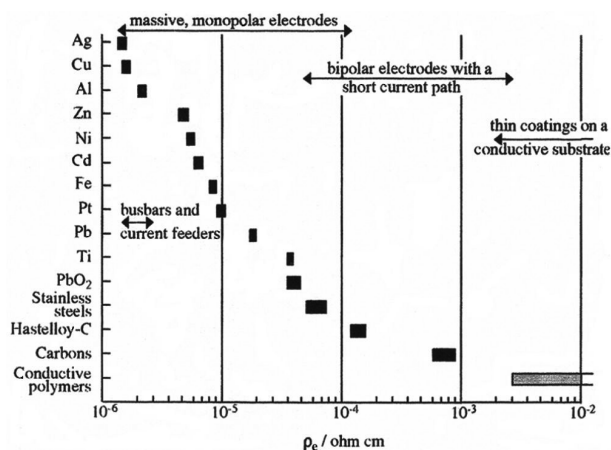

Figure 5. *Typical electrical resistivity (ρ_e) values for electrode materials*

The electrode materials must preserve their physical, mechanical, and chemical stability, often over a wide range of operating conditions. Normal process conditions may be followed or preceded by times when the cell is overdriven at a high current density to achieve higher production or zero current conditions during periods of non--use. In some cases, the electrodes may experience electrical shorting or current reversal during switch out; they must withstand alternate current (AC) ripple in the power supply. Owing to these factors and the complexity of the surface chemistry, it is important to test electrode materials under realistic process conditions for an extended period.

There are two types of electrode processes. In one case, the electrode acts only as a source or a sink of electrons, and the reaction kinetics are expected to be independent of the electrode material. In the other case, the electrode surface acts as a catalyst, and the type and rate of reaction depend critically on specific interactions between the electrode surface and electrolyte species. In the second case, dispersed microroughened surfaces are required to be used, which provides a high and active electrode area to increase the electrocatalytic effect. It should be realized that the majority of reactions lie between these two extremes. Indeed, almost all reactions, even simple redox reactions and metal depositions, show a dependence on the nature of the electrode surface.

In water electrolyzers, or FCs, an electrocatalytic electrode surface is required to promote a high rate of hydrogen evolution, or hydrogen oxidation, at a low overpotential. Alkaline water electrolyzers often make use of high-area Ni and Ni-alloy coatings, while acid electrolyte FCs where hydrogen ionizes at the anode usually employ a dispersion of platinum (Pt) and polytetrafluoroethylene

(PTFE) on a carbon substrate. Both Ni and Pt have a high exchange current density, j_0, for the H_2/H^+ couple and stabilize the adsorbed H through a mechanism that is closely related to catalytic hydrogenation.

Electrolyte phase

The electrolyte phase contains at least three essential components: the solvent, an inert (supporting) electrolyte (in high concentration), and the electroactive species (reactant).

A wide range of solvents are encountered in laboratory experiments, although factors such as cost, hazards, and recycling/disposal problems greatly limit their choice for applications in industrial electrochemical technology.[51] The solvent should generally have the following properties: (i) it must be liquid at the operational temperature, (ii) it must dissolve the electrolyte to provide a conducting solution, (iii) it must be chemically/electrochemically stable, and (iv) it must present fewer problems in storage or handling.

The importance of water as the most common solvent arises not only because of its low cost, inherent safety, and ease of handling, but also because of its following peculiar properties: (i) water is characterized by a dynamic oligomer formation via hydrogen bonding; (ii) a water molecule is small in size and has a large dipole moment, allowing it to interact electrostatically with charged species and, therefore, solvate ions readily via ion–dipole interactions; and (iii) the self-ionization of water provides a low concentration ($\approx 10^{-7}$ mol dm^{-3}) of protons and hydroxyl ions in a neutral aqueous solution. Moreover, water facilitates rapid acid-base equilibria by acting both as a proton donor and as a proton acceptor.

In general, for electrolysis to occur at a significant rate, it is essential to have a relatively high concentration of the reactant, while process economics dictate that the solvent should be stable. It is usually essential for the inert electrolyte to be dissociated extensively into cations and anions. The resulting high conductivity of the solution phase has several consequences: (i) there is a relatively low solution resistance between the electrodes, avoiding extremely high cell potential values for a given current; (ii) anions and cations of the inert electrolyte migrate and carry the majority of the current through the electrolyte, with only a very small fraction being carried by the electroactive species, implying that migration is not a significant mode of mass transfer for these species, which facilitates convective–diffusion mass transfer studies; (iii) the high ionic strength of the electrolyte results in equal and constant activity coefficients for both the reactant and the product, which simplifies Nernst equation and facilitates a treatment in terms of concentrations rather than activities; and (iv) the electrical double-layer structure is simplified, as is its influence on electrode kinetics.

Our current knowledge of liquid electrolytes largely arises from the measurements of the electrolytic conductivity, κ, which is the product of conductance, C, and a calibration factor, s, known as the cell constant. Electrolytes at a typical concentration of 1 mol dm^{-3} have k values lying within the range of 5–25 S m^{-1}, which is about six orders of magnitude smaller than most electrode materials.

The electrolytic conductivity, κ, is found to vary considerably with electrolyte concentration, c; the molar electrolytic conductivity, D, is defined as D = κ/c. The parameter D shows a dependence on concentration, and this behavior may be used to distinguish between strong (substantially dissociated) and weak (poorly dissociated) electrolytes. The fraction of charge carried by an ion is known as its transport number, denoted by the symbol t_+ for a cation and t_- for an anion. The transport number of cations tends to decrease slightly at higher concentrations of salts; the reverse trend is shown by H^+ ions in acids.

In any redox process, the thermodynamics and kinetics of charge transfer will be determined by the chemistry of the reactants and

products (as well as that of any intermediate species). For instance, taking the oxygen reduction reaction (ORR) (Eq. 6) as an example, factors leading to greater thermodynamic stability of O_2 species will discourage reduction but favor oxidation.

$$O_2 + 2 H_2O + 4 e^- \leftrightarrow 4 OH^- \qquad (6)$$

The formal potential for the O_2/OH^- couple will shift in the negative direction. Also, the structural similarity of O_2 and OH^- species will be important. For example, the reaction kinetics will be hindered by changes in the geometry, number, or type of ligands; bond lengths; and bond angles.

Separators

An ion-permeable separator (used to separate the anode from the cathode) should be incorporated only if essential. In addition to increasing the cost and complexity of cell construction, a separator increases the cell resistance substantially, thereby increasing the required cell potential for a given current density. However, a separator is useful for the following reasons: (i) the anode and cathode products may be prevented from mixing in order to maintain chemical stability or safety (e.g., explosive H_2/O_2 gas mixtures may be avoided); (ii) to a certain extent, the anode/anolyte and cathode/catholyte choices may be made independently, e.g., the anolyte may be chosen to allow the use of an inexpensive anode or to avoid a corrosive catholyte species; (iii) prevention of parasitic redox shuttle (i.e., side reactions involving reduction of a species at the cathode followed by its reoxidation at the anode) encourages a high current efficiency for the desired reactions; (iv) selective ion transport through membranes can be an essential element of the process; and (v) the separator may prevent physical contact between the anode and cathode if the electrodes are closely spaced.
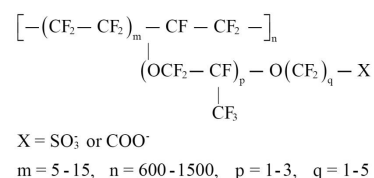
There are three main classes of separators:

1. Porous spacers are open structures, such as plastic meshes, which provide a physical barrier between electrodes. They can offer dimensional support for fragile electrodes, a membrane, or a microporous separator. Other uses include prevention of interelectrode contact (hence, electrical shorting) and promotion of turbulence next to an electrode in order to enhance mass transfer. Spacers present little or no resistance to the mixing of anolyte and catholyte, and have pore sizes in the range of 0.5–12 mm. Typical examples are shown in Figure 6.
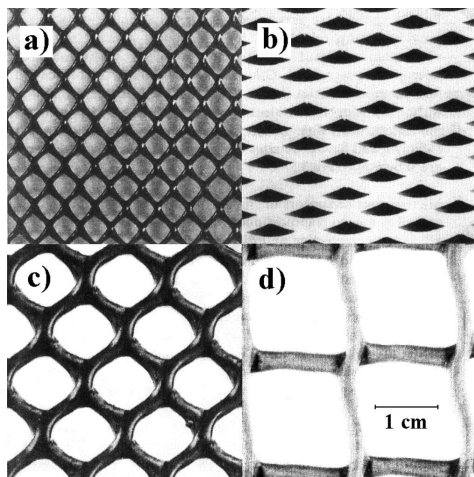
Figure 6. *Typical (polyolefin) spacers used to separate electrodes, support membranes, and promote turbulence in the electrolyte. a) Netlon greenhouse shading. b) Expamet PV 876. c) Netlon CE 121. d) Netlon garden mesh*

2. Microporous separators, or diaphragms, allow transport of solvent and solute, as well as ions, due to hydraulic permeability. However, diaphragms act as both convection and diffusion barriers because of their relatively small pore sizes (0.1–50 μm). Examples include porous ceramics (e.g., asbestos, glass frits, and porous pot) and porous polymers (e.g., porous polyvinyl chloride (PVC), polyolefins, and PTFE).

3. Ion exchange membranes divide the cell into two hydraulically separated compartments; they function as barriers to convection and diffusion, while permitting selective migration of ions. These materials have chemically designed pores of molecular size, typically in the range of 10^{-9}–10^{-8} m. Ion exchange membranes include fluorocarbon and hydrocarbon materials that have ion exchange groups distributed throughout their structure. Normally, the membrane is a thin sheet of polymer that is designed to allow passage of either anions or cations, but not both. Over the last three decades, a wide range of membranes based on perfluorinated hydrocarbon backbones have been developed (Figure 7).

$$\left[-(CF_2-CF_2)_m - CF - CF_2 - \right]_n$$
$$(OCF_2-CF)_p - O(CF_2)_q - X$$
$$CF_3$$

X = SO_3^- or COO^-

m = 5 - 15, n = 600 - 1500, p = 1-3, q = 1-5

Figure 7. *Chemical structure of a group of perfluorinated polymers used as a basis for modern cation exchange membranes*

The effective conductivity, k_{eff}, of a microporous or ion exchange membrane separator may be measured by determining the potential drop (i.e., iR_{sep}, the product of the current, i, and the resistance of the separator, R_{sep}) across a known thickness, x, of the material while operating at a fixed current density, j; that is $k_{eff} = jx/(iR_{sep})$. However, it is important to note that separators do not always show Ohmic behavior. The effective resistivity, ρ_{eff}, of the separator is the reciprocal of k_{eff}, which, after rearranging for R_{sep}, gives $R_{sep} = \rho_{eff} x/A$. Separator suppliers commonly specify the "area resistance" as the product of resistance and area, $R_{sep}A = x/k_{eff}$. Electrical resistance of the membrane is therefore minimized using a thin sheet (0.01–0.03 mm) of polymer having high ionic conductivity. Many modern membranes have an area resistance in the range of 2×10^{-5}–50×10^{-5} Ω m^2. At a j of 10^3 A m^{-2}, the potential drop across the membrane will be 0.02–0.50 V, which is often comparable to the potential drop in the catholyte or anolyte solution. The transport of species through an ion exchange membrane may be described quantitatively by a flux balance. In the case of a cation, it is given by the following expression:

migration through = migration through + convective diffusion
  the membrane   the electrolyte   in the electrolyte

$$\frac{jt_+^m}{F} = \frac{jt_+}{F} + k_m \left(c - (c)_{x=0} \right) \qquad (7)$$

where t_+ and t_+^m are the cation transport numbers in the electrolyte and the membrane, respectively; F is the Faraday's constant (96,485 C mol^{-1}); k_m is the mass transfer coefficient; and c and $(c)_{x=0}$ are concentrations of the cation in the bulk solution and at the membrane surface, respectively. If the convection–diffusion term is small, i.e., the rate of ion transport toward (or away from) the membrane surface is low, the overall reaction rate may be governed by this rate of ion transport. Important properties of ion exchange membranes for electrolytic cells are listed in Table 2.

Usually, cation exchange membranes are chemically more stable and more efficient than their anion exchange counterparts. For example, it is possible to design highly cation-selective membranes,

Table 2. Desirable properties for an ion exchange membrane to be used in an electrolytic cell

1.	High selectivity for a single type of ion (i.e., transport number ≈ 1 for such ions)
2.	Low transport of neutral molecules, including the solvent
3.	Chemical stability to the electrolyte, and to all reactants and products
4.	Mechanical stability, including strength and flexibility
5.	High ionic conductivity, but negligible electronic conductivity
6.	Ability to operate efficiently at high current densities
7.	Homogeneous structure over its whole area to promote a uniform current density
8.	Easily available and convenient to handle
9.	Relatively low cost and long lifetime

with $t_+^m > 0.95$. Unfortunately, it is difficult to achieve selectivity for a single type of cation. Instead, it is usually necessary to control the anolyte composition to have a large excess of the cation exchanging through the membrane into the catholyte.

Resistances of cell components

In previous sections, we have discussed the components of an electrolysis cell and most of the barriers or resistances that may originate during the progress of the electrolysis reactions, including electrical resistances of the circuit, activation energies of the electrochemical reactions, availability of electrode surface due to partial coverage by gas bubbles, and resistance to the ionic transfer within the electrolyte solution. The sum of all resistances found in a typical water electrolysis system is given by Eq. 8:

$$R_{total} = R_{electric} + R_{anode} + R_{bubble,O2} + R_{ions} + R_{membrane} + R_{bubble,H2} + R_{cathode} \tag{8}$$

The first resistance, $R_{electric}$, concerns the external electrical circuit resistances, including the wiring and connections at both electrodes. R_{anode} originates from the overpotential of the OER on the anode surface. $R_{bubble,O2}$ is the resistance due to partial coverage of the anode by oxygen bubbles, which hinders the contact between the anode and the electrolyte. Resistances associated with electrolyte and membrane are denoted as R_{ions} and $R_{membrane}$, respectively. Similarly, $R_{bubble,H2}$ represents the resistance generating from the obstruction of the cathode by hydrogen bubbles. $R_{cathode}$ is the resistance caused by the overpotential for the HER.

These resistances can be classified into three categories: the first category includes reaction resistances ($R_{anode} + R_{cathode}$), the second includes transport resistances ($R_{bubble,O2} + R_{ions} + R_{membrane} + R_{bubble,H2}$), and the third includes electrical resistances ($R_{electric}$).

Reaction resistances are due to the overpotentials required to overcome the activation energies of the hydrogen and oxygen formation reactions on the cathode and anode surfaces, respectively, which increase the overall cell potential directly. These are inherent energy barriers that depend on the surface activities of the employed electrodes and determine the kinetics of the electrochemical reactions.[52]

Transport resistances comprise physical resistances that account for the gas bubbles covering the electrode surface and in the electrolyte solution, and the resistances to the ionic transfer within the electrolyte and in the membrane used for separating the produced gases.

Electrical resistances can be calculated using Ohm's law. Both electrical and transport resistances cause heat generation according to Joule's law[49] and transport phenomena.[53] Energy lost due to these resistances is known as the Ohmic loss.[54]

In summary, minimization of reaction resistances requires the use of good electrocatalysts that can decrease electrode overpotentials, whereas minimization of transport and electric resistances depends on good electrochemical engineering, e.g., minimizing the interelectrode gap, ensuring that only high-ionic-conductivity materials are present between the electrodes, and ensuring that the evolved gas escapes the interelectrode gap effectively.

Clearly, the strategies to improve the energy efficiency of water electrolysis and thus the performance of the system must involve the understanding of these resistances so as to minimize them.

THERMODYNAMIC CONSTRAINTS

The thermodynamics of electrochemical cells is discussed in all textbooks of physical chemistry and electrochemistry, as are the conventions. The equilibrium or reversible cell potential is obtained[38] by subtracting the equilibrium potential of the left-hand side electrode from that of the right-hand side one (see Figure 3)

$$E_{cell}^e = E_R^e - E_L^e \tag{9}$$

and is related to the Gibbs free energy change of the overall cell reaction, ΔG_{cell}, by the following well-known equation:

$$\Delta G_{cell} = -nFE_{cell}^e \tag{10}$$

where n is the number of moles of transferred electrons. For an electrochemical cell reaction, ΔG_{cell} may be calculated as the difference between the summation of free energy values for products and reactants:

$$\Delta G_{cell} = \Sigma \Delta G_{prod} - \Sigma \Delta G_{react} \tag{11}$$

The driving force for a spontaneous cell reaction is a negative value of ΔG_{cell}, which can be written as

$$\Delta G_{cell} = \Delta H_{cell} - T\Delta S_{cell} \tag{12}$$

where ΔH_{cell} and ΔS_{cell} are, respectively, the enthalpy change and entropy change associated with the cell reaction, and T is the temperature.

For spontaneous cell reactions, $T\Delta S_{cell} > \Delta H_{cell}$, implying that $\Delta G_{cell} < 0$. E_{cell}^e for water electrolysis is −1.23 V and the free energy change is +238 kJ per mole of hydrogen.[55] Although water electrolysis converts a liquid into two gases, causing a large increase in the entropy of the system, the enthalpy value is too high (+286 kJ mol⁻¹ H$_2$ at 25 °C and 1 atm). Hence, conversion of water to hydrogen and oxygen is thermodynamically unfavorable and can occur only when enough electrical energy is supplied. Clearly, a thermodynamic discussion would lead to the conclusion that the overall cell reaction will occur and current will flow when the two electrodes of the cell are interconnected by an external electrical circuit and the cell reaction has either (i) a negative ΔG_{cell} value or (ii) a positive ΔG_{cell} value but a cell potential larger than E_{cell}^e is applied across the two electrodes to drive the chemical change. Although these conclusions are sound, they do not consider the rate at which changes can take place, i.e., the current that will flow. The rate of chemical change will depend on the kinetics of the two electrode reactions. Some reactions are inherently fast and give reasonable j values, even close to the equilibrium potential, E^e. In contrast, others are inherently slow, requiring an overpotential η (= E − E^e) to obtain any required j.[52,56] The kinetics of electrode reactions are discussed in the next section, where η can

be seen to increase with j. The extra energy requirement causes a potential drop, iR_{cell}, with i being the cell current and R_{cell} the sum of all the electrical resistances within the cell. This potential drop (or Ohmic loss) is a function of the electrolyte properties, shape of the electrodes, and cell design. The applied cell potential, E_{cell}, given by Eq. 13 is always around 1.8–2.0 V, at j values of about 1000–3000 A m^{-2}, in industrial water electrolysis systems.[57]

$$E_{cell} = E^e_{anode} - E^e_{cathode} + \sum\eta + iR_{cell} \qquad (13)$$

The total overpotential, $\sum\eta$, is the sum of the overpotentials from the HER and the OER, from the difference in electrolyte concentration, and from the formation of bubbles. Both η and iR_{cell} increase with j and may be regarded as causes of inefficiencies in the electrolysis.

There are many ways of expressing the electrolysis efficiency. The voltage efficiency of an electrolyzer can be calculated using Eq. 14.[1,58] It gives the proportion of effective voltage used to split water, from the total voltage applied to the cell, E_{cell}.

$$\%_{\text{voltage efficiency}} = (E^e_{anode} - E^e_{cathode}) / E_{cell} \times 100 \qquad (14)$$

The Faradic efficiency (Eq. 15) and the thermal efficiency (Eq. 16) are based on the energy changes of the water electrolysis reaction:

$$\eta_{Faradic} = \Delta G_{cell} / (\Delta G_{cell} + losses) = E^e_{cell} / E_{cell} \qquad (15)$$
$$\eta_{thermal} = \Delta H_{cell} / (\Delta G_{cell} + losses) = E_{tn} / E_{cell} \qquad (16)$$

where E_{tn} is the thermoneutral voltage. The Faradic efficiency considers the electrolysis reaction, while the thermal efficiency takes the whole thermal balance into account. At 25 ºC, $\eta_{Faradic}$ and $\eta_{thermal}$ are simplified into $-1.23V/E_{cell}$ and $-1.48V/E_{cell}$, respectively.

The efficiency can also be evaluated by the output of the hydrogen production rate against the total electrical energy, ΔW, applied to the electrolysis system (Eq. 17):

$$\eta_{\text{H2 production rate}} = r_{\text{H2 production rate}} / \Delta W = -V_{H2} / (iE_{cell}t) \qquad (17)$$

where t is the time and V_{H2} is the hydrogen production rate per unit volume of the cell.

From the above expressions, it is obvious that the efficiency of electrolysis can be improved by reducing the energy required to split water (by increasing the operating temperature or pressure) and/or by reducing the energy losses in the cell (by minimizing the system resistances).

RATE OF ELECTRODE PROCESSES

Overall rate of the general electrochemical reaction

$$O + ne^- \rightarrow R \qquad (18)$$

may be expressed using Faraday's laws of electrolysis. The amount of material (reactant or product) undergoing electrochemical change, m, is proportional to the amount of electrical charge, Q, involved (m = Q/nF, where the units of each side of the equation are moles). The Faraday constant, F, is equivalent to the charge associated with a mole of electrons (C mol^{-1}), i.e., it is equal to the product of the Avogadro constant, N_A, and the (fundamental) charge on a single electron, Q_e. Q is defined as the integral of cell current, i, with respect to time, t, as $Q = \int idt$; for the particular case of constant-current operation, where Q is the product of i and t, m = it/nF. Differentiating with respect to time yields dm/dt = i/nF as the expression for the rate of reaction, where dm/dt represents the rate

of reactant loss, which, for the general reaction (Eq. 18), is equal and opposite to the rate of formation of product.

As electrochemical reactions are heterogeneous surface processes, it is often convenient to relate the reaction rate to the electrode area, A, as dm/(Adt) = i/(AnF). Therefore, the expression for current density, j = i/A, may be rewritten as dm/(Adt) = j/(nF). It represents a balance at the electrode/electrolyte interface between the flux of material and the electron flux. The flux, N, may be defined formally as N = j/nF. It is also possible to present the reaction rate in terms of a unit reactor volume, V_R, as dm/($V_R$dt) = i/(nFV_R). This expresses the amount of material transformed per unit reactor volume per unit time. This quantity is usually referred to as the "space–time yield" of the reactor[59] having units of mol m^{-3} s^{-1}.

So far in this section, it has been assumed that a single reaction occurs at the electrode surface. In practice, it is important to recognize the possibility of secondary reactions, also called competing or side reactions. This may be accommodated by defining a current efficiency, f, as the fraction of electrical charge used for the primary (desired) reaction, as $\phi = Q / Q_{TOT}$, where Q_{TOT} is the total electrical charge and Q is the charge necessary for the chemical change of interest, normally calculated using Faraday's law. The current efficiency f will have values in the range $0 < \phi < 1$ (it is also often expressed as a percentage). The limits of f have the following significance: $\phi = 0$ implies that all the charge is consumed in side reactions, whereas $\phi = 1$ means that all the charge is used in producing the desired material.

In the case of constant current, ϕ may be rewritten as $= i / i_{TOT}$, where i is the partial current for the desired reaction and i_{TOT} is the total current, which allows writing the expression $dm/dt = \phi \, i_{TOT}/nF$. It is often more convenient to consider the concentration of species, c, which is the amount per unit volume of electrolyte in the reactor, V_R. In a constant-volume system, c = m/V_R.

Differentiating with respect to time gives dc/dt = dm/($V_R$dt), which may be restated as $dc/dt = \phi \, i_{TOT} / (nFV_R)$ or $dc/dt = \phi Aj_{TOT}/(nFV_R)$. This is another expression for the "space-time yield" of the reactor, which, for a given reactor volume, depends on f, the operating j, and the electrode area A. Considering the previous definition of flux N, one will get N/c = i/(nFAc); if the current is limited by the rate of convection–diffusion of reactant species to the electrode surface, i.e., under complete mass transfer control $i = i_L$, then $N_L/c = i_L/(nFAc)$, where N_L is the flux under diffusion control and i_L is the limiting diffusion current. The mass transfer coefficient, k_m, is equivalent to $i_L/(nFAc)$ and may be considered as a mass transfer flux that is normalized with respect to the bulk reactant concentration as $N_L / c = k_m$.

Following classical treatments of chemical reaction kinetics, one can write an empirical expression for the reaction rate of the form $dm/dt = kc^r$, where the rate of material change is the product of a rate constant k and the concentration raised to a power r (where r is the reaction order). However, it is important to realize that electrochemical reactions are surface processes, and it is necessary to consider material concentrations at the electrode surface (denoted by the subscript x = 0). If the reaction rate is controlled by the rate of electron transfer, one can write the rate of reduction as $dm/dt = \vec{k}(c_O)_{x=0}$ and the rate of oxidation as $dm/dt = \overleftarrow{k}(c_R)_{x=0}$.

The reaction order is assumed to be 1 with respect to the reactants for both oxidation and reduction processes. The electron transfer rate constants and strongly depend on the electrode potential, E. Empirically, the expression for the forward (reduction) process is as follows:

$$\vec{k} = \vec{k}_0 \exp\left(\frac{-\alpha_C nFE}{RT}\right) \qquad (19)$$

while that for the reverse (oxidation) process is the following:

$$\bar{k} = \bar{k}_0 \exp\left(\frac{\alpha_A nFE}{RT}\right) \qquad (20)$$

where $\vec{k}_0$ and $\bar{k}_0$ are the rate constants for reduction and oxidation, respectively, at E = 0 *vs.* the reference electrode (but because of the arbitrary choice of reference potential, they have no fundamental significance), and α_A and α_C are the anodic and cathodic transfer coefficients, respectively. These expressions are related to the control exerted by electron transfer rate on the reaction rate, which means that the electrode process is occurring at a rate lower than the rate at which reactant is supplied to the surface (or product is removed). If the reaction rate is restricted only by the rate of mass transfer of species, then it is given by the product of the mass transfer coefficient, k_m, and the bulk concentration of reactant species, c.

In many cases, both electron transfer and mass transfer contribute to the overall conversion of oxidants (O) to reductants (R). The overall reaction rate under these mixed control conditions can be expressed by Eq. 21, where c_O is the bulk concentration of oxidant species. For simplicity only the forward reaction is considered:

$$\frac{dm}{dt} = \vec{k}\, c_O\, /\left(1 + \vec{k}\,/k_m\right) \qquad (21)$$

In the absence of any net current, concentrations of O and R cannot change and the working electrode must take up the equilibrium potential for the solution. This equilibrium potential, E^e, may be measured directly or calculated from the Nernst equation (Eq. 22), where E^0 is the formal potential for the couple under consideration (i.e., the equilibrium potential when $c_R = c_O$):

$$E^e = E^0 + \frac{RT}{nF}\, \ln\, \left(c_O / c_R\right) \qquad (22)$$

The equilibrium will be dynamic, where the partial cathodic ($\vec{j}$) and partial anodic ($\bar{j}$) current densities are equal in magnitude but opposite in sign, i.e., $j = \vec{j} + \bar{j} = 0$. This dynamic equilibrium is characterized by the magnitude of the partial current densities at equilibrium, known as the exchange current density, j_0, and defined as $j_0 = -\vec{j} = \bar{j}$. This important kinetic parameter is a measure of the degree of electron transfer activity at the equilibrium potential. It is a measure of the "electrocatalytic" properties of the electrode for a given reaction and depends on the electrode material (and its surface state).

Under nonequilibrium potential conditions, the equations that best describe the current density *vs.* overpotential ($\eta = E - E^e$) under the control of electron transfer rate are the Butler-Volmer expressions:[52]

$$j = \vec{j} + \bar{j} = nF\bar{k}_0 c_R\, \exp\left(\frac{\alpha_A nFE}{RT}\right) - nF\vec{k}_0 c_O\, \exp\left(\frac{-\alpha_C nFE}{RT}\right) \qquad (23)$$

$$j = j_0\left[\exp\left(\frac{\alpha_A nF\eta}{RT}\right) - \exp\left(\frac{-\alpha_C nF\eta}{RT}\right)\right] \qquad (24)$$

These equations relate the net current density, j, to the overpotential, η, and comprise two exponential terms representing contributions from the reverse and forward processes.[31]

For a given single-step reaction (usually of a known value of n = 1) at a constant temperature, the j *vs.* η characteristics will depend on j_0, α_A, and α_C. The symmetry coefficients, α, may be regarded as the fraction of change in η that leads to a change in the rate constant for electron transfer. It is important to note that α_A and α_C are related ($\alpha_A + \alpha_C = 1$) and that, generally, $\alpha = \alpha_A \approx \alpha_C \approx \frac{1}{2}$. The j *vs.* η curves are symmetrical only about the origin for $\alpha = \frac{1}{2}$.

For large η values, the Butler–Volmer equations can be simplified to give the Tafel equations for very negative (Eq. 25) and very positive (Eq. 26) overpotentials:

$$\log j = -\log j_0 - \alpha_C n\, F\eta\, / 2.3\, RT \qquad (25)$$
$$\log j = -\log j_0 + \alpha_A n\, F\eta\, / 2.3\, RT \qquad (26)$$
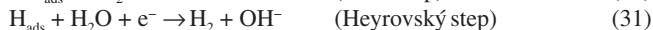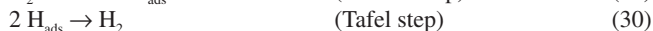
The Tafel equations can also be written as follows:

$$\left|\eta\right| = b \log j_0 + b\, \log \left|j\right| \qquad (27)$$

Under pure mass transfer control, the expression for j can be written in the form of Eq. 28, where η_{conc} is the concentration overpotential and j_L is the limiting current density, which is the current at which the surface concentration of reactant falls to the limiting case of zero:

$$j = j_L\left[1 - \exp\left(nF\eta_{conc}/RT\right)\right] \qquad (28)$$

In practice, it is common to experience a large region of η where the reaction rate is controlled partly by reactant supply and partly by electron transfer. Such reaction conditions are said to be under "mixed control." This region of mixed control will usually commence when $j = 0.05\, j_L$. The observed j is related to that for pure charge transfer control, j_{ct}, and that for pure mass transfer control, j_L, through the relationship $j^{-1} = j_{ct}^{-1} + j_L^{-1}$.

The Volmer–Tafel and Volmer–Heyrovský mechanisms are well known[1,60,61] for the HER. The first step (Eq. 29) involves the formation of adsorbed hydrogen, which is then followed by either chemical desorption (Eq. 30) or electrochemical desorption (Eq. 31), where H_{ads} is an adsorbed hydrogen atom.

$H_2O + e^- \rightarrow H_{ads} + OH^-$	(Volmer step)	(29)
$2\,H_{ads} \rightarrow H_2$	(Tafel step)	(30)
$H_{ads} + H_2O + e^- \rightarrow H_2 + OH^-$	(Heyrovský step)	(31)

The overpotential for hydrogen production, h_{H2}, is generally measured by the Tafel equation in the form of Eq. 32:

$$\eta_{H2} = [2.3RT / (\alpha_C F)] \log (j/j_0) \qquad (32)$$

where η_{H2} represents the energy barrier related to hydrogen production in the electrode. As seen before, j_0 is a function of the nature of the electrode material.[62] Hydrogen formation is intrinsically determined by the strength of the bond between hydrogen and the electrode surface. Pd has the lowest heat of adsorption of hydrogen (83.5 kJ mol^{-1}); for Ni, it is 105 kJ mol^{-1}.[63] Electrode properties, type and concentration of the electrolyte, and temperature are parameters that also influence hydrogen formation. The typical effect of temperature on η has been summarized by Kinoshita.[57]

For the HER, it is necessary to identify the rate determining step. If hydrogen adsorption (Eq. 29) is the rate determining step, electrode materials with more edges and cavities in their surface structure will favor electron transfer and create more centers for hydrogen adsorption. If hydrogen desorption (Eqs. 30 and 31) is the rate determining step, physical properties such as surface roughness or perforation will prevent bubbles from growing and increase electron transfer by adding reaction area, consequently increasing the rate of electrolysis.

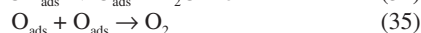An increase in the reaction overpotential may lead to a change in the HER mechanism. Therefore, the rate determining step varies depending on the applied potential range. When the overpotential is low, electron transfer is not as fast as desorption and hydrogen adsorption will be the rate determining step. In contrast, when the potential is high enough, hydrogen desorption will be the rate determining step.

The mechanism for H adsorption/desorption requires a good binding of hydrogen to the reaction site on the metal M surface, although not very strongly. Volcano plots are used to describe the variation of the exchange currents as a function of the M–H bond strength, having a maximum binding energy for Pt of about 240 kJ mol^{-1}.[64,65] The H-adsorption energy is a good parameter to identify the most promising materials for the HER. The HER exchange current of Pt in acid media is at least 2 orders of magnitude higher than that in alkaline electrolytes, including KOH. This is due to the shorter Pt–H$_{ads}$ distance in alkaline media, as suggested by theoretical estimates.[66] It has been claimed that Ni(OH)$_2$ nanoclusters on Pt surface enhance HER rates in 0.1 M KOH by 1 order of magnitude,[67] although no theoretical explanation for this synergistic effect has been attempted. The long-term stability of Ni(OH)$_2$ in the strongly reducing environment occurring at the cathode is also not discussed.

By alloying metals (e.g., Ni) having higher energy than optimal H-bond energy with those (e.g., Mo) having lower energy, it is expected that the turnover rate of the reaction centers and the intrinsic catalytic activity will increase. Evidence for these synergistic effects was somewhat vague until recently, owing to the fact that some of the materials were characterized poorly and the theoretical analyses were not sufficiently comprehensive.[68]

Relating catalytic activity with electronic structure computation is a challenging task, but the density functional theory (DFT) has now allowed crucial advances in the area of electrocatalysis, in particular concerning synergistic effects. For example, it has recently been confirmed experimentally through a large-scale combinatorial screening that BiPt alloy is a better HER catalyst at pH 0 than Pt.[69] In addition, MoS$_2$ nanoparticles were proposed as a low-cost replacement of Pt as a HER catalyst in acidic solutions,[70] with both DFT simulations and experiments proving that the performance of MoS$_2$ nanoparticles could be beaten only by Pt group metal catalysts. Amorphous MoS$_3$ has recently been shown to perform better than crystalline MoS$_2$ in the same conditions,[71] although its practical use is still far from reality. There are numerous studies in the open literature devoted to the development of new electrocatalysts for the HER, but their practical application is limited by the prevailing trial-and-error approach and the lack of long-term stability measurements.[68]

The pathways for the OER mechanism are a bit more complex than those suggested for the HER. There is some controversy in the literature, but the most generally accepted mechanism for the OER[72] is that described by Eqs. 33–35:

$$OH^- \rightarrow OH_{ads} + e^- \tag{33}$$
$$OH^- + OH_{ads} \rightarrow O_{ads} + H_2O + e^- \tag{34}$$
$$O_{ads} + O_{ads} \rightarrow O_2 \tag{35}$$

One of the charge transfer steps (Eqs. 33 and 34) is the rate controlling step. A slow electron transfer step determines the reaction at low temperatures. On the other hand, a slow recombination step (Eq. 35) controls the reaction at high temperatures on Ni electrode.[72,73] Fe and Ni alloys have been found to be able to reduce the oxygen overpotential to some extent.[74]

The reaction rate decreases with increasing activation energy, E_a; therefore, reducing E_a is crucial for more efficient water electrolysis. In general, E_a increases with j, but it can be lowered using appropriate electrocatalysts.[42] The overpotential for oxygen evolution is more difficult to reduce than that for hydrogen evolution, because of its complex mechanism and irreversibility.

It is generally believed that few noble metal compounds are thermodynamically stable at a low pH and high potential. Nevertheless, acid solutions or PEMs have been considered as electrolytes in water electrolyzers because acidic media show high ionic conductivity and are free from carbonate formation, as compared with alkaline electrolytes.[75]

Noble metals as electrocatalysts for OER in acidic media were initially examined by polarization techniques. Ruthenium (Ru) and iridium (Ir) showed high activity toward OER, but metallic elements were passivated immediately when they reached higher anodic potentials.[76–81] Then again, metal oxides were of interest because the oxide layer anodically grown on the metal surface is less stable than that formed by other procedures. A thick film of ruthenium oxide (RuO$_2$) fabricated on the substrate as a dimensionally stable anode (DSA) in water electrolyzers exhibited high electrocatalytic activity, depending on adsorption of chemical species, concentration of intermediates, and morphology.[82–84] However, it was pointed out that the formation of ruthenium tetroxide (RuO$_4$) by further oxidation of rutile RuO$_2$ during anodic processes increases kinetic losses at the anode significantly. In contrast, iridium oxide (IrO$_2$) films were very stable even at potentials close to 2 V, despite showing higher overpotential for OER than RuO$_2$ films. IrO$_2$ shows higher stability and preferentially evolves molecular oxygen rather than being oxidized further.[85] To obtain synergistic effects from different metal oxides, a variety of mixed metal oxides were developed. Ruthenium–iridium oxide showed improved electronic properties and suppressed the formation of RuO$_4$; alloying the above two metals with tantalum (Ta) enhanced OER kinetics and the addition of tin (Sn) resulted in a metastable mixed oxide.[86,87] Recently, Ru-rich Pt electrocatalysts and titanium (Ti)- or titanium carbide (TiC)-supported electrocatalysts for OER have been suggested.[88,89]

Bifunctional electrocatalysts, which can work for both oxygen evolution and oxygen reduction, have also been proposed for water electrolysis. A typical bifunctional electrocatalyst is composed of a noble metal oxide such as IrO$_2$. For unsupported bifunctional electrocatalysts, Pt–MO$_x$ (M = Ru, Ir, Na), bimetallic (e.g., Pt–Ir), and trimetallic (e.g., Pt$_{4.5}$Ru$_4$Ir$_{0.5}$) materials have been developed.[90–93] On the other hand, to enhance the electrochemical surface area and electronic properties of the anode, several supported bifunctional electrocatalysts have been proposed, with IrO$_2$-supported Pt electrocatalysts, for example, demonstrating high electrocatalytic activity toward OER.[94] Significant advances in the development of novel OER electrocatalysts have been made, but considerable challenges still remain, particularly concerning catalysts' cost and durability.

The water electrolyzer potential accounts for both anode and cathode reactions. The overpotentials from hydrogen and oxygen evolutions are the main sources of reaction resistances. The other obvious resistance at high current densities is the Ohmic loss in the electrolyte, which includes resistances from the bubbles, diaphragm, and ionic transfer. Identifying these resistances is vital to enhance the efficiency of water electrolysis.

RESISTANCES IN THE SYSTEM

Electrical resistances lead to energy waste in the form of heat generation, according to Ohm's law. The electrical resistances in a water electrolysis system have three main components: (i) resistances in the system circuits; (ii) mass transfer phenomena, including ion transfer within the electrolyte; and (iii) gas bubbles covering the electrode surfaces and the diaphragm.

Resistances in the circuit are determined by the type and dimension of the material, its preparation method, and the conductivity of each individual component of the circuit, including wires, connectors, and electrodes. These resistances can be reduced by decreasing the length of the wire, increasing its cross-sectional area, and adopting more conductive wire materials.

Ionic transfer within the electrolyte depends on the electrolyte concentration, distance between electrodes, and membrane. Ionic

resistance can be minimized by changing the electrolyte concentration or adding appropriate additives to increase its conductivity. Presence of bubbles in the electrolyte and on the electrode surface also causes additional resistances to the ionic transfer and electrochemical reactions.

The effective resistance of the membrane, used to separate the produced hydrogen and oxygen gases, is generally 3–5 times higher than the resistance of an equivalent thickness of electrolyte solution.[59] Energy losses in the electrical circuit are always relatively small, but those due to ionic transfer become more significant at higher current densities. Formation of gas bubbles on the electrode surface contribute significantly to the total energy loss.

Convective mass transfer also controls ionic transfer, heat dissipation and distribution, and the action of bubbles in the electrolyte. The viscosity and flow of the electrolyte play important roles in mass transfer, temperature distribution, and size, detachment, and rising velocity of bubbles, in turn influencing the current and potential distribution in the electrolysis cell. The concentration of the electrolyte increases as the electrolysis progresses, leading to an increase in the solution viscosity. Water is usually added continuously to the system to maintain a constant electrolyte concentration and thus a constant viscosity.

Better mass transfer leads to higher reaction rates, but not necessarily to increased hydrogen production. A higher reaction rate generates larger amounts of gas bubbles, which can hinder the contact between the electrode and the electrolyte. Mechanical recirculation of the electrolyte solution accelerates the detachment of gas bubbles and brings them to the gas collectors. Electrolyte recirculation is also important to prevent concentration gradients in the cell and distribute heat evenly within the electrolyte. At the startup, electrolyte recirculation can be used to heat up the electrolyte to the operating temperature, usually 80-90 °C.[57,95]

Considering that the bubble phenomenon is the major source of electrical resistances in the cell, minimizing its effect is critical to improve the electrolyzers' efficiency. During electrolysis, hydrogen and oxygen gas bubbles are formed on the surfaces of the cathode and anode, respectively, and are detached from the surface only when they grow big enough. The bubbles' coverage reduces the contact between the electrolyte and the electrode, thereby blocking electron transfer and increasing the Ohmic loss of the whole system. Detachment of the bubbles also depends on the electrode wettability, i.e., on the electrolyte replacement at the electrode/electrolyte interface.[96,97] Appropriate coatings can be applied on the electrode surface to make it more hydrophilic, thereby reducing the surface coverage by gas bubbles. Another approach is based on the addition of surfactants to the electrolyte solution to reduce its surface tension and facilitate detachment of bubbles from the electrodes. In summary, the bubble effect is a problem that has always to be dealt with, by modifying the electrode surface, reducing the electrolyte surface tension, or using mechanical fluid circulation to force the gas bubbles to leave the cell. Much work has been devoted to the bubble behavior in electrolysis systems,[96,98–101] but further studies are still required to minimize its negative effects.

SOME PRACTICAL CONSIDERATIONS

To compare different water electrolysis systems, it is necessary to discuss a number of practical parameters relevant to the performance of water electrolyzers, including electrolysis cell configuration, operating conditions, and a few external requirements.

Regarding the cell configuration, electrolyzers may be constructed in either unipolar or bipolar design (Figure 8). A unipolar (or "tank--type") electrolyzer (Figure 8a) consists of alternate positive and negative electrodes held apart by porous separators, i.e., membranes. Positive electrodes are all coupled together in parallel, as are the negative electrodes, and the whole assembly is immersed in a single electrolyte bath ("tank") to form a unit cell. A plant-scale electrolyzer is then built up by connecting these units electrically in series. The total voltage applied to the whole electrolysis cell is the same as that applied to the individual unit cells.
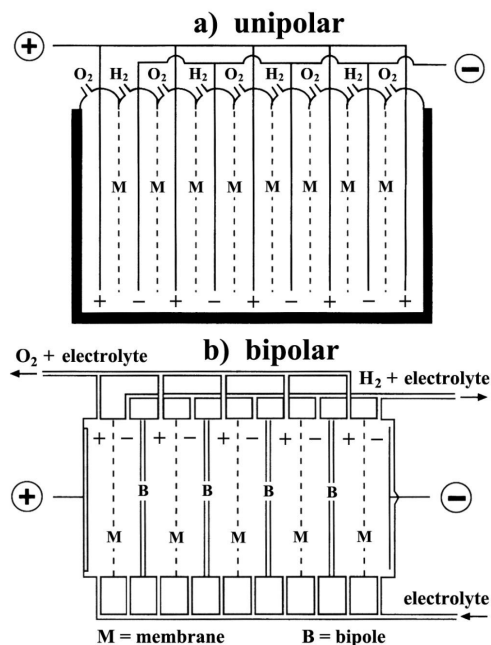

Figure 8. *Electrolyzer modules with a) unipolar and b) bipolar cell configurations*

On the other hand, in a bipolar electrolyzer a metal sheet (or "bipole") connects electrically adjacent cells in series. As seen in Figure 8b, the electrocatalyst for the negative electrode is coated on one face of the bipole and that for the positive electrode of the adjacent cell is coated on the reverse face. In this case, the total cell voltage is the sum of the individual unit cell voltages. Therefore, a series-connected stack of such cells forms a module that operates at a higher voltage and lower current than the tank-type (unipolar) design. To meet the requirements of a large electrolysis plant, these modules are connected in parallel so as to increase the current.

These two different cell configurations present different electrode reactions. For the unipolar configuration, the same electrochemical reaction (either the HER or the OER) occurs on both sides of each electrode. On the other hand, in the bipolar configuration, two different reactions (HER and OER) take place simultaneously on the opposite sides of each electrode not directly connected to the power source. This means that one side of each electrode acts as a cathode and the other as an anode (although both sides are at the same potential), with the exception of the two end electrodes that are connected to the DC power source. The resulting cell voltage for these two basic configurations is quite different. For typical industrial processes, the unipolar configuration presents a cell voltage of about 2.2 V and the bipolar configuration has a value of $2.2 \times (n - 1)$ V (where n is the number of electrodes).[1]

Owing to the simplicity of the unipolar configuration, this type of electrolyzer is easy to fabricate and requires low maintenance, but presents high electrical currents at low voltages, causing large Ohmic losses. On the other hand, the bipolar configuration has lower Ohmic losses in the electrical circuit connectors; however, it demands much higher precision in its design and manufacturing to prevent electrolyte and gas leakage between cells.[1]

The gap between electrodes must also be considered during cell design.[102] It corresponds to the distance that the ions have to travel within the electrolyte.[103] A smaller gap has the advantage of less resistance to ionic transportation. However, if the gap is too small, it can induce electric sparks, posing an explosion hazard. An optimum electrode gap must be identified for each particular cell.

The electrolyte flow forces convective mass transfer in the cell. At high current densities, electrochemical reactions are limited by the electrolyte mass transfer. Stirring and/or inducing turbulence reduces the concentration gradients in the electrolyte and enhances mass transfer.

An electrolyzer's operating cell voltage is directly related to its energy consumption and electrical efficiency. The cell is considered inefficient if a higher voltage is required to produce an equivalent hydrogen mass, while keeping the current constant. The operating current density also defines the electrolyzer's energy efficiency. Conventional water electrolyzers generally run at current densities ranging from 1000 to 3000 A m^{-2}. The current density determines the rate of hydrogen production, with higher current densities leading to higher rates of the electrochemical reactions. However, fast bubble formation resulting from an increased rate of gas production also increases the overpotential due to the bubbles' resistance. Therefore, current density should be kept within a certain range, with compromises between the gas production rates and the energy efficiency.

The operating temperature is another important parameter. Conventional alkaline water electrolyzers are designed to run at temperatures of around 80-90 °C. Increasing the operating temperature has the advantage of decreasing the equilibrium cell voltage. However, high temperatures increase water loss due to evaporation and require highly resistant materials to maintain the equipment's structural integrity.[57] Also, heat management and the material required for making the diaphragm bring more engineering issues at higher operating temperatures.

The pressure at which the electrolyzer operates should depend on the end use of the produced hydrogen. Cells operating at an elevated pressure of 3.5 MPa reduce bubble sizes, thereby minimizing the Ohmic losses. However, the efficiency of pressurized cells is not significantly superior to that of ambient pressure cells.[43] Moreover, these cells work with higher proportions of dissolved gas, requiring a more endurable diaphragm.

The type and concentration of the electrolyte defines the ionic conductivity of the solution and, consequently, the ionic transfer in the cell. KOH (25-30 wt.%) is adopted widely in commercial electrolyzers.[104] It is essential for the electrode materials to be stable in highly corrosive alkaline environments, to minimize the electrolyzer's operation and maintenance costs. Noble metals have good resistance to corrosion by alkalis and high electrocatalytic activity, but are too expensive for widespread applications in water electrolysis.[38] Transition metals such as iron and copper have good electrocatalytic activity but are less resistant to alkali attack. Ni is considered to be one of the best electrode materials for alkaline water electrolysis, with both good resistance to alkali attack and high electrocatalytic activity, while not being too expensive.

The function of the membrane is to separate the produced hydrogen and oxygen gases while still allowing ionic transfer. Globally, the benefits of separating the gases compensate for the Ohmic resistance caused by the presence of a diaphragm. Current research on separators for alkaline water electrolyzers is directed toward the development of new materials with low electrical resistance and high corrosion stability.[105]

Water quality is a central factor to ensure long-life operation of an electrolyzer. Impurities can accumulate in the cell, and deposit on the electrode surface and in the membrane, thus hindering mass and charge transfer.[106] The highly alkaline environment in the electrolysis cell requires the concentrations of magnesium and calcium ions to be sufficiently low to avoid precipitation of their hydroxides. Deposition of these compounds is ruled by the solubility product constant (K_{sp}), which is the limiting value for precipitation to occur.[31] When the concentration of these impurities reaches this value, deposition takes place. In addition, when the current density exceeds the so-called limiting current of hydroxyl ions,[107] chloride ions present in solution are oxidized to chlorine at the anode surface, which is extremely corrosive to most metallic components of the electrolyzer.

Electrolyzers of different scales are designed to meet the different needs for hydrogen. Commercially, an electrolyzer can vary from several kW to several hundred MW in terms of power consumption.[43,108] Electrolyzer technologies can be compared in terms of their energy efficiency or hydrogen production efficiency. For low-temperature alkaline water electrolysis, a net efficiency, η_{net}, of around 50% is considered to be good.[109] On the other hand, $\eta_{H2yield}$ is useful when considering hydrogen production per unit volume at a unit time; a value of about 2.3 m^3 m^{-3} h^{-1} kWh^{-1} is typical for a unipolar water electrolyzer.[43]

In terms of safety, the whole system, including the membrane, should be designed carefully keeping in mind the flammability of hydrogen and oxygen mixtures. Also, due to the corrosive nature of the alkaline electrolyte, leakage may occur at the connections and seals of the electrolyzer. The bipolar cell configuration, having a more complex design, poses a higher risk of electrolyte leakage than the unipolar configuration.

Materials used for cell construction determine the durability of the electrolyzer. These materials should be resistant to highly alkaline electrolytes. Since corrosion is normally more severe at the joints and connections, joint sealant materials must be stable under the operating conditions.[110]

FUTURE TRENDS

As shown in previous sections, water splitting is one of the most significant reactions in electrochemistry, being involved in numerous applications, namely those concerning electrochemical energy storage and conversion.[52,111,112] Considering that electrode reactions are the major causes of energy losses, the exact mechanism of the electrochemical processes has been pursued consistently for years,[113–116] to allow designing of highly efficient electrolytic cells, necessarily with better electrocatalysts.[117] However, the conventional theories in electrochemistry,[52] such as the Gouy-Chapman theory, the Nernst equation, and the Butler-Volmer model, do not fully allow the atomic-level understanding of the HER/OER at the electrolytic cell. In particular, the detailed mechanism of electrocatalysis has been extremely difficult to analyze, mainly because of the complex nature of the geometric and electronic structures of electrodes and solution.[65,118] Therefore, it has been realized that rigorous quantum mechanical (QM) treatment is essential to obtain reliable energetics for electrochemical reactions. QM treatment of the electrochemical interface, based on both computational facilities and theoretical models,[119–121] enables a better understanding of the electrolytic processes, where the electrochemical potentials, water environment, and electrodes are all taken into account explicitly. Accordingly, many studies are progressively revealing the atomic-level details of the electrode reactions at water electrolysis cells.[122–125]

Early electrolysis cells were about 60-75% efficient. However, the current small-scale, best-practice figure is close to 80-85%, with larger units being a little less efficient (ca. 70-75%). However, it should be noted that when electricity generated from thermal power stations is used, the overall efficiency is only about 25-30% for the conversion

of fossil fuel to hydrogen. This is not a very attractive return on the invested energy. Nevertheless, R&D efforts add continuous innovations to the existing concepts of water electrolysis. Most of the recent research is focused on reducing system resistances and, consequently, energy losses.[28,126] In this way, one would approach the final goal of "manufacturing" hydrogen as a clean and economic energy carrier.

Truly clean hydrogen can be obtained only through the use of renewable energy forms. This can be accomplished by photochemical water splitting or through intermediate production of electricity, using wind resources or PV cells, followed by water electrolysis. Use of artificial photosynthetic systems poses one of the major challenges in the field of chemistry.[127] The simplest and practical approach to produce solar fuels using artificial photosynthetic systems is to mimic the natural photosynthetic process. Light harvesting leads to charge separation, followed by charge transport to deliver the oxidizing and reducing equivalents to catalytic sites where evolution of hydrogen and oxygen occurs.

Figure 9 presents the basic features of an artificial photosynthetic system:[128] (i) an antenna for light harvesting, (ii) a reaction center for charge separation, (iii) catalysts as interfaces between the charge-separated state and the substrate, and (iv) a membrane to provide physical separation of the products.
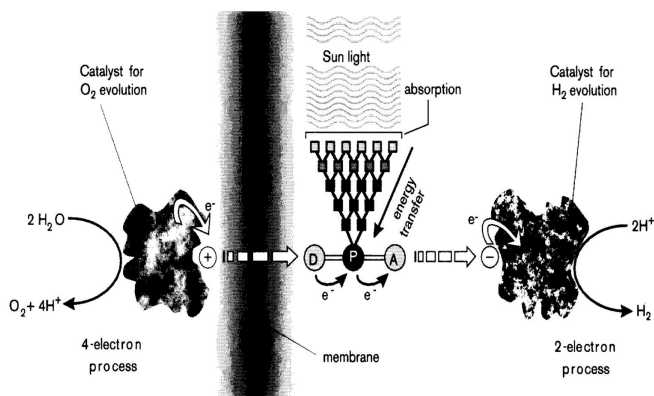

Figure 9. *Basic features of an artificial photosynthetic system*[128]

Complexity of the natural photosynthetic systems is largely related to their living nature. It is known that single photosynthetic functions, such as photoinduced energy and electron transfer, can be copied by simple artificial systems. However, nature tells us that efficient conversion of light into chemical energy requires the involvement of supramolecular structures with precise organization in the dimensions of space (relative location of the components), energy (excited-state energies and redox potentials), and time (rates of competing reactions). This organization is a result of natural evolution and is dictated by complex intermolecular interactions. Its transposition to artificial systems can be imposed by molecular engineering using covalent or noncovalent bonding.[129]

Although progresses have been accomplished in each individual component of artificial photosynthesis used for the cleavage of water into hydrogen and oxygen, integration of those components in a working system has not yet been achieved. Nevertheless, photochemical conversion of solar power into electrical power is now possible using PV cells and photoelectrochemical (PEC) cells.[130-133]

PV cells capture photons by exciting electrons across the band gap of a semiconductor. This process generates electron–hole pairs that are separated subsequently, typically by p–n junctions introduced by doping.[134] In the n-type regions of the device, conduction-band electrons can flow easily to and from cell contacts, whereas valence holes cannot; the p-type regions have the opposite properties. Such

an asymmetry causes a flow of photogenerated electrons and holes in opposite directions, generating a potential difference at the external electrodes. First-generation PV cells, which account for 85% of the current market,[135] are based on expensive polycrystalline silicon wafers. Less expensive PV modules have efficiencies of 15–20% and a lifetime of the order of 30 years.[134] However, for solar electricity to be cost competitive with fossil-based electricity at utility scale, manufacturing costs must be reduced substantially. This goal has been reached partially with second-generation cells, which are based on thin films of less expensive materials such as amorphous or nanocrystalline Si, CdTe, or $CuInSe_2$. However, further research is needed to improve the efficiency of these cells in order to make them economically competitive.

A practical method for applying PV electrolysis was first reported by Fujishima and Honda in 1972.[136] A titanium dioxide (TiO_2) electrode captures the energy of ultraviolet (UV) light and converts it into electricity, which is to be used in the direct decomposition of water into hydrogen and oxygen. With the increasing interest in renewable energies, PV electrolysis has become a major contributor to hydrogen production. A PV electrolysis system includes a PV cell and an electrolysis circuit. The photoelectrodes absorb energy from UV light and release electricity required for water splitting. Much research is currently devoted to developing photoelectrochemically active semiconductor materials. The low efficiency of the PV electrolysis (~2-6%) prevents its use for large-scale hydrogen production.[137] Low solar energy density, variations in energy content of solar radiation, low operating current density, and expensive and unstable electrode materials make large-scale application of PV electrolysis infeasible at this stage.[138]

PEC cells, also known as dye-sensitized solar cells or Grätzel cells,[139] are based on the sensitization of wide band gap semiconductors by dyes capable of using solar energy (i.e., visible light). Although the basic principles of dye sensitization of semiconductors have long been established,[140] the application of such techniques to light–energy conversion became appealing only after new nanocrystalline semiconductor electrodes of very high surface area had been developed.[141,142]

The working principle of a dye-sensitized solar cell is shown in Figure 10.[139] The system comprises a photosensitizer S linked in some way (usually, by –COOH, $-PO_3H_2$, or $-B(OH)_2$ functional groups) to the semiconductor surface, a solution containing a redox mediator A, and a metallic counter electrode.
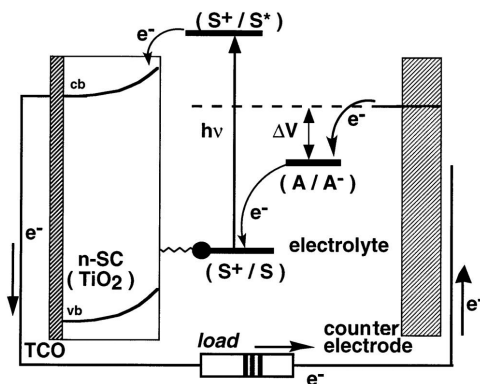

Figure 10. *Example of a dye-sensitized solar cell*[139]

The sensitizer is first excited by light absorption. The excited sensitizer then injects, in the femto- to pico-second timescale, an electron into the conduction band of the semiconductor. The oxidized sensitizer is reduced by a relay molecule, which then diffuses to discharge at a conductive glass counterelectrode. As a result, a

photopotential is generated between the two electrodes under open--circuit conditions, and a corresponding photocurrent can be obtained on closing the external circuit by an appropriate load. Therefore, the main difference of PEC cells from photosynthetic systems is that the redox potential energy of the charge-separated state is not stored in products of subsequent reactions, rather it is used directly to produce a photocurrent.[143,144]

High-temperature electrolysis (HTE), also known as steam electrolysis, is performed using a solid oxide electrolysis cell (SOEC), as shown in Figure 11. It adopts a solid oxide, as the electrolyte, in a process that is essentially the reverse operation of a solid oxide FC.
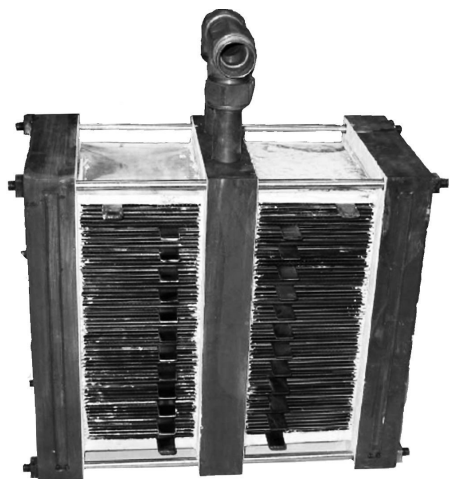

Figure 11. *Example of an SOEC stack*

An SOEC operates at elevated temperatures, typically between 500 and 850 ºC, where water splitting is favored thermodynamically.[145] Steam passes through the cathode side of the solid electrolyte where the water gas molecules are reduced to hydrogen, releasing oxide ions in the process (Eq. 37). These oxide ions migrate through the electrolyte to the anode side where they combine to form oxygen molecules, releasing electrons[145,146] (Eq. 38).

Cathode $H_2O + 2 e^- \rightarrow H_2 + O^{2-}$ (37)

Anode $O^{2-} \rightarrow \frac{1}{2} O_2 + 2 e^-$ (38)
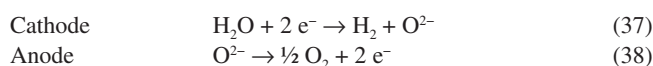
Hydrogen production via the SOEC generally involves consumption of less electrical energy than conventional low-temperature water electrolyzers, owing to the improved thermodynamic and kinetic operating conditions at high temperatures.[147] For instance, for an average current density of 7000 A m^{-2} and an inlet steam temperature of 750 ºC, the electrical energy consumption of the stack will be around 3 kWh per normal m^3 of hydrogen, which is significantly less than the energy consumption of a typical low-temperature alkaline water electrolyzer (4.5 kWh).[148] However, it should be emphasized that this comparison does not take into account the circulation and losses of heating energy. Moreover, HTE must also address stricter temperature control and safety issues, as well as use of appropriate construction materials.[149–153]

Although alkaline water electrolysis is undergoing continuous improvement, it may currently be seen as a mature technology, with reasonable efficiency when compared to other emergent water electrolysis systems. Although PEM electrolyzers have high efficiencies, they need to overcome several technical hitches. PV electrolysis faces many engineering challenges concerning its scale up. An SOEC has to deal with corrosion issues because of its high operating temperature. It seems that improving the low-temperature alkaline water electrolysis

technology, to increase its efficiency, is still a more realistic solution for large-scale hydrogen production in the near future.[154] For the widespread commercial application of alkaline water electrolysis, current research trends are particularly focusing on the electrodes, electrolytes, ionic transport, and bubble formation.

Ni is the most widely used electrode material for water electrolysis because of its good stability and electrocatalytic activity. However, deactivation of the electrode material is a major problem in electrolysis, and even Ni is affected by it. Ni electrode deactivation is caused by the high hydrogen concentration near the electrode, which leads to the formation of a Ni hydride phase at the surface. Iron coatings are known to inhibit the formation of the Ni hydride phase and hence prevent electrode deactivation.[39] Dissolved vanadium species have the ability to activate Ni cathodes during hydrogen evolution in alkaline media.[155]

Electrode materials affect the activation energy of the electrochemical reaction. Electrocatalysts are used to facilitate the charge transfer and/or to enhance the rate of the chemical reactions. They reduce the activation energy of the process by decreasing the associated overpotential. The effect of the electrocatalyst depends on the electronic structure of the electrode. Ni, Pd, and Pt with d^{8}s^2, d^{10}s^0, and d^{9}s^1 electronic configurations, respectively, exhibit minimum η values for the HER. In contrast, Zn, Cd, and Hg with d^{10}s^2 electronic configuration show the maximum values. The spillover theory in electrocatalysis, by Bockris et al.,[1] explains the interactions between substances.

The Brewer–Engel valence bond theory has also been used intensively to study hydrogen electrodes. Jaksic has reported[156–158] that by alloying metals of the left half of the transition series in the periodic table with empty or less filled d-orbitals with metals of the right half of the series with more filled d-bands, maximum bond strength and stability of the intermetallic alloy phases could be achieved. This leads to a well-pronounced synergism in electrocatalysis. It is implied that some of the electrons of the metal with more filled d-bands are shared with the metal with less filled or empty d-orbitals.[156,157] The observed synergistic effect normally exceeds the performance of the individual parent metals and approaches reversible behavior within a wide range of current densities.

Therefore, alloys formed by metals with different electronic distributions are adopted to improve the electrocatalytic activity of electrodes.[159–168] Santos et al. studied hydrogen discharge using platinum–rare earth (Pt–RE) alloys (RE = Ho, Sm, Ce, Dy) and found out that Pt–RE alloys of equiatomic compositions exhibit superior performances than single Pt electrodes.[167,168] Cathodes containing Pt–Mo alloys also presented much higher activities than those containing individual parent metals.[169] A composite cathode of Ni, Fe, and Zn, prepared by electrodeposition, showed good stability for up to 200 h at a current density of 1350 A cm^{-2}. This composite also presented good activity in 28% KOH, at 80 ºC; its overpotential was ~100 mV, which is significantly lower than that of mild steel (~400 mV).[170]

Noble metal oxides are commonly used as electrocatalysts. Ruthenium dioxide (RuO$_2$), iridium dioxide (IrO$_2$), and mixed oxides containing these two noble metals have been proved to have high electrocatalytic activity for the OER.[171–177] Ir$_x$Ru$_y$Ta$_z$O$_2$ as an anode electrocatalyst achieved an overall cell voltage of 1.57 V at 1 A cm^{-2} at 80 °C, with an energy consumption of 3.75 kWh N m^{-3} H$_2$ and efficiency of 94%, for a total noble metal loading of less than 2.04 mg cm^{-2}.[47] However, there are some non-noble, less expensive metals that also present electrocatalytic activity and are being introduced for use in oxygen[178–185] and hydrogen[165,166,186–191] evolution reactions. Additionally, during designing an electrode, it is normally doped or coated with more stable and active layers. The doping material may be chosen from a wide range of metals.[192] For example, Li doping

increases the electrical conductivity of the electrode material and also its roughness factor (when adding up to 3% Li), favoring the OER.[193] A single-cell electrolyzer using a Li-doped Co_3O_4 anode electrocatalyst exhibited a current density of 300 mA cm^{-2} at a voltage of 2.05 V at 45 ºC. The $Li_{0.21}Co_{2.79}O_4$ anode showed good stability in continuous operation for 10 h at 300 mA cm^{-2} and 30 °C.[194]

Nanostructured electrodes present an enlarged surface area and possess unique electronic properties. The increased active area of the nanostructured electrode reduces the operating current density of the electrolyzer. A 25% reduction in overpotential and 20% reduction in energy consumption were achieved by the use of a Ru nanorod cathode when compared to a regular planar Ru cathode.[55] This improvement can be ascribed to the increased active area of the nanostructured electrode, which reduced the operating current density of the electrolyzer. Kamat[132] proposed the use of nanostructures to improve the performance of photoelectrolysis by enhancing charge transfer, which also have the potential to be applied as electrodes for water electrolysis.

Regarding the electrolyte, and as seen before, most commercial electrolyzers have adopted alkaline solutions of KOH or NaOH. However, energy consumption during water electrolysis may be reduced significantly by adding small quantities of activating compounds.[195,196] Ionic liquids (ILs) are organic compounds that are liquid at room temperature; these consist only of cations and anions, and thus possess reasonably high ionic conductivity and stability.[197] Imidazolium ILs have been used as electrolyte media for hydrogen production through water electrolysis. Current densities up to 200 A m^{-2} and efficiencies higher than 94.5% have been achieved using imidazolium ILs in conventional electrochemical cells with Pt electrodes at room temperature and atmospheric pressure.[198] The main problem with ILs is that they normally have high viscosity and low water solubility.[51,199,200] This hinders mass transfer, and leads to low current densities and, consequently, low hydrogen production rates. ILs with higher conductivities and better water solubility are required to enhance ionic transfer and improve the water electrolysis process.

Research efforts on new electrolyte media for water electrolysis are still relatively scarce when compared to the huge number of studies devoted to the development of new electrocatalytic materials. There is an immense potential for improving overall electrolysis efficiency using electrolyte additives, which can enhance mass transfer and thus reduce the electrolyte resistance. Addition of electrolyte additives also affects the affinity between the electrolyte and the electrodes, facilitating bubble management.

As discussed before, formation and transportation of bubbles cause considerable Ohmic losses in the cell. The dissolved gas bubbles and the gas interfaces between electrodes and electrolyte generate large resistances to water electrolysis. The bubble phenomena have been studied intensively,[96,201,202] but no mechanisms or models have yet been applied to alkaline water electrolysis. The contributions of the electrode surface coverage by gas bubbles and the electrolyte-phase bubble void fraction to the Ohmic drop have been discussed.[97] Reducing the bubbles' residence time on the electrode surface is fundamental to minimize their size and thus reduce their resistance.

Hydrophilic electrodes have higher affinity to water than to gas bubbles. Their application facilitates mass transfer from the electrolyte to the electrode. Surfactants may be added to the electrolyte to reduce the surface tension. This will decrease bubbles' size and accelerate their detachment from the electrode surface. The added surfactants must be inert to the electrochemical reactions[203] and stable during the whole process.

The electrode surface may also be modified mechanically by introducing slits and holes on it to promote the escape of the gas bubbles. To avoid gas trapping in the holes, the typical diameter for electrode perforation in alkaline water electrolysis is 0.1 and 0.7 mm for hydrogen and oxygen, respectively.[38]

Forced mechanical circulation of the electrolyte solution can also help sweeping the bubbles off the electrode's surface. The electrolyte circulation speed should be high enough to promote mass transfer and eliminate concentration gradients.

In summary, the overall performance of novel electrolyzers is impressive, particularly regarding their high operating current densities and relatively low cell voltages, and further improvements are expected to occur.

CONCLUSIONS

Alkaline water electrolysis, powered by renewable energy sources (e.g., sun, wind, and waves), can be integrated into a distributed energy system to produce hydrogen for end use or as an energy storage medium. Compared to the current major methods used for hydrogen production, alkaline water electrolysis is generally seen as a simpler technology; however, it still needs much work to improve its present efficiency. Further research is required to overcome durability and safety issues that still block the widespread use of alkaline water electrolysis.

The fundamentals of water electrolysis have been examined and performances of various water electrolysis designs have been compared. Thermodynamic and kinetic approaches to the alkaline water electrolysis technology have been envisaged. The resistances that hinder the electrolysis efficiency have been identified, which include resistances generated by gas bubbles, activation energies of electrochemical reactions, mass transfer, and electrical resistances in the circuit. The effect of the bubbles' resistance can be minimized by modifying the electrode and/or using electrolyte additives. The reaction overpotential may be adjusted by the choice of a suitable electrode material. Mass transfer resistances can be reduced substantially through electrolyte circulation. A clear awareness of the involved resistances is vital to improve the electrolyzer's efficiency, especially when working at high current densities.

Some practical considerations on the electrolyzers' development indicate that alkaline water electrolysis is a viable method for hydrogen production. The historical background of water electrolysis technology has been presented to shed light on what should be the future trends to follow. To improve the efficiency of alkaline water electrolysis further, R&D efforts focusing on the development of new electrocatalysts and effective electrolyte additives, use of physical/chemical electrode modifications, and appropriate management of the gas bubble phenomena are urgently required.

ACKNOWLEDGMENTS

REFERENCES

1. Bockris, J. O'M.; Conway, B. E.; Yeager, E.; White, R. E.; *Comprehensive treatise of electrochemistry*; Plenum Press: New York, 1981.
2. Turner, J. A.; *Science* **1999**, *285*, 687.
3. Mueller-Langer, F.; Tzimas, E.; Kaltschmitt, M.; Peteves, S.; *Int. J. Hydrogen Energy* **2007**, *32*, 3797.
4. Veziroğlu, T. N.; *Conversion to Hydrogen Economy, Electronic Newsletter of the International Association for Hydrogen Energy*; IAHE: Vol. 5, Issue 2, Fall 2012.

5. Steinfeld, A.; *Int. J. Hydrogen Energy* **2002**, *27*, 611.

6. Bockris, J. O'M.; *Int. J. Hydrogen Energy* **2002**, *27*, 731.

7. Bockris, J. O'M.; Veziroglu, T. N.; *Int. J. Hydrogen Energy* **2007**, *32*, 1605.

8. Barreto, L.; Makihira, A.; Riahi, K.; *Int. J. Hydrogen Energy* **2003**, *28*, 267.

9. Ramachandran, R.; Menon, R. K.; *Int. J. Hydrogen Energy* **1998**, *23*, 593.

10. Lattin, W. C.; Utgikar, V. P.; *Int. J. Hydrogen Energy* **2007**, *32*, 3230.

11. Eliezer, D.; Eliaz, N.; Senkov, O. N.; Froes, F. H.; *Mater. Sci. Eng. A* **2000**, *280*, 220.

12. Eliaz, N.; Eliezer, D.; Olson, D. L.; *Mater. Sci. Eng., A* **2000**, *289*, 41.

13. Pletcher, D.; Li, X.; *Int. J. Hydrogen Energy* **2011**, *36*, 15089.

14. Turner, J. A.; *Science* **2004**, *305*, 972.

15. Rosen, M. A.; Scott, D. S.; *Int. J. Hydrogen Energy* **1998**, *23*, 653.

16. Trommer, D.; Noembrini, F.; Fasciana, M.; Rodriguez, D.; Morales, A.; Romero, M.; Steinfeld, A.; *Int. J. Hydrogen Energy* **2005**, *30*, 605.

17. Momirlan, M.; Veziroglu, T. N.; *Renewable Sustainable Energy Rev.* **2002**, *6*, 141.

18. Sato, S.; Lin, S. Y.; Suzuki, Y.; Hatano, H.; *Fuel* **2003**, *82*, 561.

19. Stojić, D. Lj.; Marčeta, M. P.; Sovilj, S. P.; Miljanić, S. S.; *J. Power Sources* **2003**, *118*, 315.

20. Trasatti, S.; *J. Electroanal. Chem.* **1999**, *476*, 90.

21. Dunn, S.; *Int. J. Hydrogen Energy* **2002**, *27*, 235.

22. De Souza, R. F.; Padilha, J. C.; Goncalves, R. S.; De Souza, M. O.; Rault-Berthelot, J.; *J. Power Sources* **2007**, *164*, 792.

23. Hollmuller, P.; Joubert, J. M.; Lachal, B.; Yvon, K.; *Int. J. Hydrogen Energy* **2000**, *25*, 97.

24. Varkaraki, E.; Lymberopoulos, N.; Zachariou, A.; *J. Power Sources* **2003**, *118*, 14.

25. Barbir, F.; *Solar Energy* **2005**, *78*, 661.

26. Oi, T.; Sakaki, Y.; *J. Power Sources* **2004**, *129*, 229.

27. Kato, T.; Kubota, M.; Kobayashi, N.; Suzuoki, Y.; *Energy* **2005**, *30*, 2580.

28. Zeng, K.; Zhang, D.; *Prog. Energy Combust. Sci.* **2010**, *36*, 307.

29. De Levie, R.; *J. Electroanal. Chem.* **1999**, *476*, 92.

30. Kreuter, W.; Hofmann, H.; *Int. J. Hydrogen Energy* **1998**, *23*, 661.

31. Rieger, P. H.; *Electrochemistry,* 1st ed., Prentice-Hall: New Jersey, 1987.

32. *The production of hydrogen and oxygen through the electrolysis of water*; in *Scientific American Supplement*, Vol. XXXII, no. 819: New York, 1891.

33. Bowen, C. T.; Davis, H. J.; Henshaw, B. F.; Lachance, R.; Leroy, R. L.; Renaud, R.; *Int. J. Hydrogen Energy* **1984**, *9*, 59.

34. Rosa, V. M.; Santos, M. B. F.; Da Silva, E. P.; *Int. J. Hydrogen Energy* **1995**, *20*, 697.

35. Hickner, M. A.; Ghassemi, H.; Kim, Y. S.; Einsla, B. R.; McGrath, J. E.; *Chem. Rev.* **2004**, *104*, 4587.

36. Divisek, J.; Mergel, J.; Schmitz, H.; *Int. J. Hydrogen Energy* **1990**, *15*, 105.

37. Sequeira, C. A. C.; Santos, D. M. F.; *Ciência & Tecnologia dos Materiais* **2010**, *22*, 76.

38. Wendt, H.; Kreysa, G.; *Electrochemical engineering*, 1st ed., Springer-Verlag: Berlin, Heidelberg, 1999.

39. Mauer, A. E.; Kirk, D. W.; Thorpe, S. J.; *Electrochim. Acta.* **2007**, *52*, 3505.

40. Bocca, C.; Barbucci, A.; Cerisola, G.; *Int. J. Hydrogen Energy* **1998**, *23*, 247.

41. Soares, D. M.; Teschke, O.; Torriani, I.; *J. Electrochem. Soc.* **1992**, *139*, 98.

42. Leroy, R. L.; *Int. J. Hydrogen Energy* **1983**, *8*, 401.

43. Pletcher, D.; Walsh, F. C.; *Industrial electrochemistry,* 2nd ed., Blackie Academic & Professional: London, 1990.

44. Lu, P. W. T.; Srinivasan, S.; *J. Appl. Electrochem.* **1979**, *9*, 269.

45. Sequeira, C. A. C.; Santos, D. M. F., eds.; *Polymer electrolytes: fundamentals and applications*; Woodhead Publishing Ltd: Cambridge, 2010.

46. Grigoriev, S. A.; Porembsky, V. I.; Fateev, V. N.; *Int. J. Hydrogen Energy* **2006**, *31*, 171.

47. Marshall, A.; Borresen, B.; Hagen, G.; Tsypkin, M.; Tunold, R.; *Energy* **2007**, *32*, 431.

48. Janjua, M. B. I.; Leroy, R. L.; *Int. J. Hydrogen Energy* **1985**, *10*, 11.

49. Oldham, K. B.; Myland, J. C.; *Fundamentals of electrochemical science*, 1st ed., Academic Press: San Diego, 1993.

50. Berndt, D.; Spahrbier, D. In *Ullmann's Encyclopedia of Industrial Chemistry*; Wiley-VCH: Weinheim, 2005.

51. Sequeira, C. A. C.; Santos, D. M. F.; *J. Braz. Chem. Soc.* **2009**, *20*, 387.

52. Bard, A. J.; Faulkner, L. R.; *Electrochemical methods fundamentals and applications*, 2nd ed., John Wiley & Sons: New York, 2001.

53. Bird, R. B.; Stewart, W. E.; Lightfoot, E. N.; *Transport phenomena*, 2nd ed., John Wiley & Sons: New York, 2007.

54. Belmont, C.; Girault, H.; *J. Appl. Electrochem.* **1994**, *24*, 475.

55. Kim, S.; Koratkar, N.; Karabacak, T.; Lu, T. M.; *Appl. Phys. Lett.* **2006**, *88*, 263106.

56. Rossmeisl, J.; Logadottir, A.; Norskov, J. K.; *Chem. Phys.* **2005**, *319*, 178.

57. Kinoshita, K.; *Electrochemical oxygen technology*, 1st ed., John Wiley & Sons: New York, 1992.

58. Bloom, H.; Futmann, F.; *Electrochemistry: the past thirty and the next thirty years*, 1st ed., Plenum Press: New York, 1977.

59. Pickett, D. J.; *Electrochemical reactor design*, 2nd ed., Elsevier: Amsterdam, 1979.

60. Santos, D. M. F.; Sequeira, C. A. C.; Lobo, R. F. M.; *Int. J. Hydrogen Energy* **2010**, *35*, 9901.

61. Sequeira, C. A. C.; Santos, D. M. F.; Sousa, J. R.; Brito, P. S. D.; *Mater. Technol.* **2009**, *24*, 119.

62. Newman, J. S.; *Electrochemical systems*; Prentice Hall: New Jersey, 1991.

63. Trasatti, S.; *J. Electroanal. Chem.* **1971**, *33*, 351.

64. Trasatti, S.; *J. Electroanal. Chem.* **1972**, *39*, 163.

65. Sequeira, C. A. C.; *Ciência & Tecnologia dos Materiais* **2012**, *24*, 99.

66. Sheng, W.; Gasteiger, H. A.; Shao-Horn, Y.; *J. Electrochem. Soc.* **2010**, *157*, B1529.

67. Subbaraman, R.; Tripkovic, D.; Strmcnik, D.; Chang, K.-C.; Uchimura, M.; Paulikas, A. P.; Stamenkovic, V.; Markovic, N. M.; *Science* **2011**, *334*, 1256.

68. Marini, S.; Salvi, P.; Nelli, P.; Pesenti, R.; Villa, M.; Berrettoni, M.; Zangari, G.; Kiros, Y.; *Electrochim. Acta* **2012** *82*, 384.

69. Greeley, J.; Jaramillo, T. F.; Bonde, J.; Chorkendorff, I.; Nørskov, J. K.; *Nat. Mater.* **2006**, *5*, 909.

70. Jaramillo, T. F.; Jørgensen, K. P.; Bonde, J.; Nielsen, J. H.; Horch, S.; Chorkendorff, I.; *Science* **2007**, *317*, 100.

71. Vrubel, H.; Merki, D.; Hu, X.; *Energy Environ. Sci.* **2012**, *5*, 6136.

72. Sequeira, C. A. C.; Santos, D. M. F.; Cameron, E.; Brito, P. S. D.; *Mater. Technol.* **2008**, *23*, 142.

73. Cappadonia, M.; Divisek, J.; von der Heyden, T.; Stimming, U.; *Electrochim. Acta* **1994**, *39*, 1559.

74. Potvin, E.; Brossard, L.; *Mater. Chem. Phys.* **1992**, *31*, 311.

75. Park, S.; Shao, Y.; Liu, J.; Wang, Y.; *Energy Environ. Sci.* **2012**, *5*, 9331.

76. Damjanovic, A.; Dey, A.; Bockris, J. O'M.; *J. Electrochem. Soc.* **1966**, *113*, 739.

77. Miles, M. H.; Thomason, M. A.; *J. Electrochem. Soc.* **1976**, *123*, 1459.

78. Conway, B. E.; *Prog. Surf. Sci.* **1995**, *49*, 331.

79. Trasatti, S.; *Electrochim. Acta* **2000**, *45*, 2377.

80. Gottesfeld, S.; Srinivasan, S.; *J. Electroanal. Chem.* **1978**, *86*, 89.

81. Mozota, J.; Vukovic, M.; Conway, B. E.; *J. Electroanal. Chem.* **1980**, *114*, 153.

82. Galizzioli, D.; Tantardini, F.; Trasatti, S.; *J. Appl. Electrochem.* **1974**, *4*, 57.

83. Galizzioli, D.; Tantardini, F.; Trasatti, S.; *J. Appl. Electrochem.* **1975**, *5*, 203.

84. Lodi, G.; Sivieri, E.; De Battisti, A.; Trasatti, S.; *J. Appl. Electrochem.* **1978**, *8*, 135.

85. Song, S.; Zhang, H.; Ma, X.; Shao, Z.; Baker, R. T.; Yi, B.; *Int. J. Hydrogen Energy* **2008**, *33*, 4955.

86. Yeo, R. S.; Orehotsky, J.; Visscher, W; Srinivasan, S.; *J. Electrochem. Soc.* **1981**, *128*, 1900.

87. Hutchings, R.; Muller, K.; Kötz, F.; Stucki, S.; *Journal Of Materials Science* **1984**, *19*, 3987.

88. Boodts, J. F. C.; Trasatti, S.; *J. Electrochem. Soc.* **1990**, *137*, 3784.

89. Neyerlin, K. C.; Bugosh, G., Forgie, R.; Liu, Z.; Strasser, P.; *J. Electrochem. Soc.* **2009**, *156*, B363.

90. Swette, L. L.; LaConti, A. B.; McCatty, S. A.; *J. Power Sources* **1994**, *47*, 343.

91. Ioroi, T.; Kitazawa, N.; Yasuda, K.; Yamamoto, Y.; Takenaka, H.; *J. Electrochem. Soc.* **2000**, *147*, 2018.

92. Chen, G.; Delafuente; D. A.; Sarangapani, S.; Mallouk, T. E.; *Catal. Today* **2001**, *67*, 341.

93. Rivas, S.; Arriaga, L. G.; Morales, L.; Fernández, A. M.; *Int. J. Electrochem. Sci.* **2012**, *7*, 3601.

94. Yao, W.; Yang, J.; Wang, J.; Nuli, Y.; *Electrochem. Commun.* **2007**, *9*, 1029.

95. Dyer, C. K.; *J. Electrochem. Soc.* **1985**, *132*, 64.

96. Kiuchi, D.; Matsushima, H.; Fukunaka, Y.; Kuribayashi, K.; *J. Electrochem. Soc.* **2006**, *153*, E138.

97. Matsushima, H.; Nishida, T.; Konishi, Y.; Fukunaka, Y.; Ito, Y.; Kuribayashi, K.; *Electrochim. Acta* **2003**, *48*, 4119.

98. Vogt, H.; Balzer, R. J.; *Electrochim. Acta* **2005**, *50*, 2073.

99. Hine, F.; Yasuda, M.; Nakamura, R.; Noda, T.; *J. Electrochem. Soc.* **1975**, *122*, 1185.

100. Dejonge, R. M.; Barendrecht, E.; Janssen, L. J. J.; Vanstralen, S. J. D.; *Int. J. Hydrogen Energy* **1982**, *7*, 883.

101. Boissonneau, P.; Byrne, P.; *J. Appl. Electrochem.* **2000**, *30*, 767.

102. Pletcher D.; Li, X; Wang, S.; *Int. J. Hydrogen Energy* **2012**, *37*, 7429.

103. Nunes, S. P.; Peinemann, K. V.; *Membrane technology*, 2ⁿᵈ ed., Wiley-VCH Verlag GmbH & KGaA: Weinheim, 2007.

104. Gutmann, F.; Murphy, O. J.; *Modern aspects of electrochemistry*; Plenum Press: New York, 1983.

105. Vermeiren, Ph.; Adriansens, W.; Moreels, J. P.; Leysen, R.; *Int. J. Hydrogen Energy* **1998**, *23*, 321.

106. Millet, P.; Andolfatto, F.; Durand, R.; *Int. J. Hydrogen Energy* **1996**, *21*, 87.

107. Krstajic, N.; Popovic, M.; Grgur, B.; Vojnovic, M.; Sepa, D.; *J. Electroanal. Chem.* **2001**, *512*, 27.

108. Schiller, G.; Henne, R.; Mohr, P.; Peinecke, V.; *Int. J. Hydrogen Energy* **1998**, *23*, 761.

109. *The hydrogen economy*; Engineering NAo.: N. R. Council, 2005.

110. Divisek, J.; Malinowski, P.; Mergel, J.; Schmitz, H.; *Int. J. Hydrogen Energy* **1988**, *13*, 141.

111. Fang, Y.-H.; Liu, Z.-P.; *Sci. China: Chem.* **2010**, *53*, 543.

112. Bockris, J. O'M.; *Int. J. Hydrogen Energy* **1999**, *24*, 1.

113. Lasia, A.; In *Handbook of fuel cells: fundamentals, technology, applications, vol. 2*; Vielstich, W.; Lamm, A.; Gasteiger, H. A., eds.; John Wiley & Sons Ltd.: Chichester, 2003.

114. Seong, S; Anderson, A. B.; *J. Phys. Chem.* **1996**, *100*, 11744.

115. Damjanovic, A.; Dey, A; Bockris, J. O'M.; *Electrochim. Acta* **1966**, 11, 791.

116. Trasatti, S.; *Electrochim. Acta* **1984**, *29*, 1503.

117. Hammer, B.; Norskov, J. K.; *Adv. Catal.* **2000**, *45*, 71.

118. Kolasinski, K. W.; *Surface science: foundations of catalysis and nanoscience, 3ʳᵈ ed.*; John Wiley & Sons Ltd.: Chichester, UK, 2012.

119. Darling, G. R.; Holloway, S.; *Rep. Prog. Phys.* **1995**, *58*, 1595.

120. Hammer, B.; Norskov, J. K.; *Surf. Sci.* **1995**, *343*, 211.

121. Parr, P.; Yang, W.; *Density functional theory of atoms and molecules*; Oxford University Press: Oxford, 1989.

122. Anderson, A. B.; Neshev, N. M.; Sidik, R. A.; Shiller, P.; *Electrochim. Acta* **2002**, *47*, 2999.

123. Taylor, C. D.; Kelly, R. G.; Neurock, M.; *J. Electroanal. Chem.* **2007**, *607*, 167.

124. Rossmeisl, J.; Qu, Z. W.; Zhu, H.; Kroes, G. J.; Norskov, J. K.; *J. Electroanal. Chem.* **2007**, *607*, 83.

125. Cai, Y; Anderson, A. B.; *J. Phys. Chem. B* **2005**, *109*, 7557.

126. Nikolic, V. M.; Tasic, G. S.; Maksic, A. D.; Saponjic, D. P.; Miulovic, S. M.; Marceta Kaninski, M. P.; *Int. J. Hydrogen Energy* **2010**, *35*, 12369.

127. Collings, A. F.; Critchley, C., eds.; *Artificial photosynthesis. From basic biology to industrial application*, 1ˢᵗ ed., Wiley-VCH: Weinheim, 2005.

128. Balzani, V.; Credi, A.; Venturi, M.; *Curr. Opin. Chem. Biol.* **1997**, *1*, 506.

129. Balzani, V.; Scandola, F.; *Comprehensive supramolecular chemistry, vol. 10.* Atwood, J. L.; Davies J. E. D.; MacNicol, D. D.; Vögtle, F., eds.; Pergamon Press: Oxford, 1996.

130. Lewis, N. S.; Nocera, D. G.; *Proc. Natl. Acad. Sci. U.S.A.* **2006**, *103*, 15729.

131. Lewis, N. S.; *Science* **2007**, *315*, 798.

132. Kamat, P. V.; *J. Phys. Chem. C* **2007**, *111*, 2834.

133. Youngblood, W. J.; Anna Lee, S.-H.; Maeda, K.; Mallouk, T. E.; *Acc. Chem. Res.* **2009**, *42*, 1966.

134. Green, M. A.; *Third generation photovoltaics: advanced solar energy generation*; Springer-Verlag: Berlin, 2003.

135. Private communication; Office of Science, US Department of Energy, Washington, DC, 2013.

136. Fujishima, A.; Honda, K.; *Nature* **1972**, *238*, 37.

137. Gibson, T. L.; Kelly, N. A.; *Int. J. Hydrogen Energy* **2008**, *33*, 5931.

138. Holladay, J. D.; Hu, J.; King, D. L.; Wang, Y.; *Catal. Today* **2009**, *130*, 244.

139. Kalyanasundaram, K.; Grätzel, M.; *Coord. Chem. Rev.* **1998**, *177*, 347.

140. Gerischer, H.; Willig, F.; *Top. Curr. Chem.* **1976**, *61*, 31.

141. Hagfeldt, A.; Grätzel, M.; *Acc. Chem. Res.* **2000**, *33*, 269.

142. Kisch, H.; Macyk, W.; *ChemPhysChem* **2002**, *3*, 399.

143. Maeda, K.; Teramura, K.; Lu, D.; Takata, T.; Saito, N.; Inoue, Y.; Domen, K.; *Nature* **2006**, *440*, 295.

144. Sayama, K.; Mukasa, K.; Abe, R.; Abe, Y.; Arakawa, H.; *Chem. Commun.* **2001**, 2416.

145. Udagawa, J.; Aguiar, P.; Brandon, N. P.; *J. Power Sources* **2008**, *180*, 354.

146. Brisse, A.; Schefold, J.; Zahid, M.; *Int. J. Hydrogen Energy* **2008**, *33*, 5375.

147. Utgikar, V.; Thiesen, T.; *Int. J. Hydrogen Energy* **2006**, *31*, 939.

148. Udagawa, J.; Aguiar, P.; Brandon, N. P.; *J. Power Sources* **2007**, *166*, 127.

149. Perfiliev, M. V.; *Int. J. Hydrogen Energy* **1994**, *19*, 227.

150. Liepa, M. A.; Borhan, A.; *Int. J. Hydrogen Energy* **1986**, *11*, 435.

151. Quandt, K. H.; Streicher, R.; *Int. J. Hydrogen Energy* **1986**, *11*, 309.

152. Matsumoto, H.; Okubo, M.; Hamajima, S.; Katahira, K.; Iwahara, H.; *Solid State Ionics* **2002**, *152-153*, 715.

153. Nikiforov, A. V.; Petrushina, I. M.; Christensen, E.; Alexeev, N. V.; Samokhin, A. V.; Bjerrum, N. J.; *Int. J. Hydrogen Energy* **2012**, *37*, 18591.

154. Pettersson, J.; Ramsey, B.; Harrison, D.; *J. Power Sources* **2006**, *157*, 28.

155. Abouatallah, R. M.; Kirk, D. W.; Thorpe, S. J.; Graydon, J. W.; *Electrochim. Acta* **2001**, *47*, 613.

156. Jaksic, M. M.; *Electrochim. Acta* **1984**, *29*, 1539.

157. Jaksic, M. M.; *Int. J. Hydrogen Energy* **1987**, *12,* 727.

158. Jaksic, M. M.; *J. Mol. Catal.* **1986**, *38*, 161.

159. Rosalbino, F.; Macciò, D.; Angelini, E.; Saccone, A.: Delfino, S.; *J. Alloys Compd.* **2005**, *403*, 275.

160. Dos Santos Andrade, M.H.; Acioli, M.L.; Da Silva Jr., J.G.; Silva, J.C.P.; Vilar, E.O.; Tonholo, J.; *Int. J. Hydrogen Energy* **2004**, *29*, 235.

161. Crnkovic, F. C.; Machado, S. A. S.; Avaca, L. A.; *Int. J. Hydrogen Energy* **2004**, *29*, 249.

162. Sheela, G.; Pushpavanam, M.; Pushpavanam, S.; *Int. J. Hydrogen Energy* **2002**, *27*, 627.

163. Sequeira, C. A. C.; Santos, D. M. F.; Brito, P. S. D.; *Energy* **2011**, *36*, 847.

164. Rosalbino, F.; Macciò, D.; Saccone, A.; Angelini, E.; Delfino, S.; *J. Alloys Compd.* **2007**, *431*, 256.

165. Rosalbino, F.; Macciò, D.; Saccone, A.; Angelini, E.; Delfino, S.; *Int. J. Hydrogen Energy* **2011**, *36*, 1965.

166. Rosalbino, F.; Macciò, D.; Angelini, E.; Saccone, A.; Delfino, S.; *Int. J. Hydrogen Energy* **2008**, *33*, 2660.

167. Santos, D. M. F.; Šljukić, B.; Sequeira, C. A. C.; Macciò, D.; Saccone, A.; Figueiredo, J. L.; *Energy* **2013**, *50*, 486.

168. Santos, D. M. F.; Sequeira, C. A. C.; Macciò, D.; Saccone, A.; Figueiredo, J. L.; *Int. J. Hydrogen Energy* **2013**, *38*, 3137.

169. Stojić, D. Lj.; Grozdić, T. D.; Marčeta Kaninski, M. P.; Maksić, A. D.; Simić, N. D.; *Int. J. Hydrogen Energy* **2006**, *31*, 841.

170. Giz, M. J.; Bento, S. C.; Gonzalez, E. R.; *Int. J. Hydrogen Energy* **2000**, *25*, 621.

171. Ma, H.; Liu, C.; Liao, J.; Su, Y.; Xue, X.; Xing, W.; *J. Mol. Catal. A: Chem* **2006**, *247*, 7.

172. Lee, Y.; Suntivich, J.; May, K. J.; Perry, E. E.; Shao-Horn, Y.; *J. Phys. Chem. Lett.* **2012**, *3*, 399.

173. Lyons, M. E. G.; Floquet, S.; *Phys. Chem. Chem. Phys.* **2011**, *13*, 5314.

174. Guerrini, E.; Chen, H.; Trasatti, S.; *J. Solid State Electrochem.* **2007**, *11*, 939.

175. Ye, F.; Li, J.; Wang, X.; Wang, T.; Li, S.; Wei, H.; Li, Q.; Christensen, E.; *Int. J. Hydrogen Energy* **2010**, *35*, 8049.

176. Marshall, A. T.; Sunde, S.; Tsypkin, M.; Tunold, R.; *Int. J. Hydrogen Energy* **2007**, *32*, 2320.

177. Chen, X.; Chen, G.; *Electrochim. Acta* **2005**, *50*, 4155.

178. Komo, M.; Hagiwara, A.; Taminato, S.; Hirayama, M.; Kanno, R.; *Electrochemistry* **2012**, *80*, 834.

179. Li, X.; Walsh, F. C.; Pletcher, D.; *PCCP* **2011**, *13*, 1162.

180. Kubisztal, J.; Budniok, A.; *Int. J. Hydrogen Energy* **2008**, *33*, 4488.

181. Cibrev, D.; Jankulovska, M.; Lana-Villarreal, T.; Gómez, R.; *Int. J. Hydrogen Energy* **2013**, *38*, 2746.

182. Singh, R. N.; Kumar, M.; Sinha, A. S. K.; *Int. J. Hydrogen Energy* **2012**, *37*, 15117.

183. Singh, R. N.; Madhua; Awasthi, R.; Tiwari, S. K.; *Int. J. Hydrogen Energy* **2009**, *34*, 4693.

184. Singh, R. N.; Singh, J. P.; Singh, A.; *Int. J. Hydrogen Energy* **2008**, *33*, 4260.

185. Singh, R. N.; Singh, J. P.; Lal, B.; Thomas, M. J. K.; Bera, S.; *Electrochim. Acta* **2006**, *51*, 5515.

186. Rosalbino, F.; Delsante, S.; Borzone, G.; Angelini, E.; *Int. J. Hydrogen Energy* **2008**, *33*, 6696.

187. Solmaz, R.; Döner, A.; Şahin, I.; Yüce, A. O.; Kardaş, G.; Yazici, B.; Erbil, M.; *Int. J. Hydrogen Energy* **2009**, *34*, 7910.

188. Jacques, P.-A.; Artero, V.; Pécautb, J.; Fontecave, M.; *Proc. Nat. Acad. Sci. USA* **2009**, *106*, 20627.

189. Lin, T.-W.; Liu, C.-J.; Lin, J.-Y.; *Appl. Catal. B* **2013**, *134-135*, 75.

190. Wang, C.; Li, W.; Lu, X.; Xie, S.; Xiao, F.; Liu, P.; Tong, Y.; *Int. J. Hydrogen Energy* **2012**, *37*, 18688.

191. Herraiz-Cardona, I.; Ortega, E.; Vázquez-Gómez, L.; Pérez-Herranz, V.; *Int. J. Hydrogen Energy* **2012**, *37*, 2147.

192. Wu, X.; Scott, K.; *J. Mater. Chem.* **2011**, *21*, 12344.

193. Hamdani, M.; Pereira, M. I. S.; Douch, J.; Addi, A. A.; Berghoute, Y.; Mendonca, M. H.; *Electrochim. Acta* **2004**, *49*, 1555.

194. Wu, X.; Scott, K.; *Int. J. Hydrogen Energy* **2013**, *38*, 3123.

195. Stojić, D. Lj.; Grozdić, T. D.; Marčeta Kaninski, M. P.; Stanić, V. D.; *Int. J. Hydrogen Energy* **2007**, *32*, 2314.

196. Marčeta Kaninski, M. P.; Maksić, A. D.; Stojić, D. Lj.; Miljanić, S. S.; *J. Power Sources* **2004**, *131*, 107.

197. Endres, F.; El Abedin, S. Z.; *PCCP* **2006**, *8*, 2101.

198. De Souza, R. F.; Padilha, J. C.; Goncalves, R. S.; Rault-Berthelot, J.; *Electrochem. Commun.* **2006**, *8*, 211.

199. Santos, D. M. F.; Sequeira, C. A. C.; *Int. J. Hydrogen Energy* **2010**, *35*, 9851.

200. Sequeira, C. A. C.; Pardal, T. C. D.; Santos, D. M. F.; Condeço, J. A. D.; Franco, M. A. W.; Gonçalves, M. C. M. R.; *ECS Trans.* **2007**, *3/18*, 37.

201. Jones, S. F.; Evans, G. M.; Galvin, K. P.; *Adv. Colloid Interface Sci.* **1999**, *80*, 27.

202. Vogt, H.; *Electrochim. Acta* **1989**, *34*, 1429.

203. Wei, Z. D.; Ji, M. B.; Chen, S. G.; Liu, Y.; Sun, C. X.; Yin, G. Z.; Shen, P. K.; Chan, S. H.; *Electrochim. Acta* **2007**, *52*, 3323.